ACS NANO

www.acsnano.org

REVIEW

Flexible Metasurfaces for Multifunctional Interfaces

Yunlei Zhou, Shaolei Wang, Junyi Yin, Jianjun Wang, Farid Manshaii, Xiao Xiao, Tianqi Zhang, Hong Bao, Shan Jiang,* and Jun Chen*

Cite This: *ACS Nano* 2024, 18, 2685−2707

Read Online

ACCESS | Metrics & More | Article Recommendations

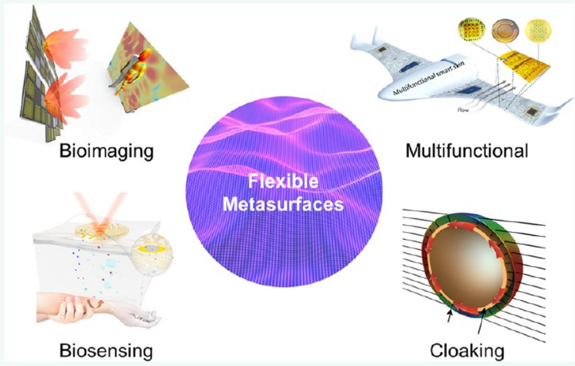

ABSTRACT: **Optical metasurfaces, capable of manipulating the properties of light with a thickness at the subwavelength scale, have been the subject of extensive investigation in recent decades. This research has been mainly driven by their potential to overcome the limitations of traditional, bulky optical devices. However, most existing optical metasurfaces are confined to planar and rigid designs, functions, and technologies, which greatly impede their evolution toward practical applications that often involve complex surfaces. The disconnect between two-dimensional (2D) planar structures and three-dimensional (3D) curved surfaces is becoming increasingly pronounced. In the past two decades, the emergence of flexible electronics has ushered in an emerging era for metasurfaces. This review delves into this cutting-edge field, with a focus on both flexible and conformal design and fabrication techniques. Initially, we reflect on the milestones and trajectories in modern research of optical metasurfaces, complemented by a brief overview of their theoretical underpinnings and primary classifications. We then showcase four advanced applications of optical metasurfaces, emphasizing their promising prospects and relevance in areas such as imaging, biosensing, cloaking, and multifunctionality. Subsequently, we explore three key trends in optical metasurfaces, including mechanically reconfigurable metasurfaces, digitally controlled metasurfaces, and conformal metasurfaces. Finally, we summarize our insights on the ongoing challenges and opportunities in this field.**

KEYWORDS: *metasurfaces, nanophotonics, optics, metamaterials, curved surfaces, flexible electronics, conformal designs, smart skins, multifunctional interfaces*

1. INTRODUCTION

Flexible, wearable, and conformal electronics are one of the fastest-growing trends in devices today, and they are revolutionizing people's way of life. These electronics, especially prominent in bioelectronics and healthcare, boast a variety of applications. They can be mounted on the skin, attached to clothes, or even implanted into the body. Examples include epidermal,[1−9] wearable,[10−19] and implantable bioelectronics.[20−24] These devices enable continuous, noninvasive monitoring of vital physiological signals in real time, comfortably providing clinically relevant information for disease diagnosis, preventive healthcare, and rehabilitation.[25−36] These devices are particularly promising for managing chronic diseases like cardiovascular issues, metabolic disorders, and diabetes, which are of significant in an aging population.[37−45] During health crises like the COVID-19 pandemic, they can reduce the need for hospital visits and readmissions.[46] Beyond bioelectronics, the versatility of flexible electronics extends to wearable energy harvesters,[47−56] robotic skins for haptic interfaces,[57−62] and smart skins for aircraft to measure aerodynamic parameters *in situ*.[63−65] The trend towards flexible electronics is also evident in fields like photonics,[66] acoustics,[67,68] metamaterials,[69] and etc. These devices are ultrathin, low-modulus, and lightweight, making them "mechanically invisible" when applied to objects with arbitrary surfaces.[70−79] Propelled by advancements in materials and manufacturing technologies, we are making significant strides in this era of flexible, wearable, and conformal devices.

Metasurfaces are two-dimensional metamaterials that exhibit extraordinary physical properties (such as optical, acoustic,

Received: September 26, 2023
Revised: January 11, 2024
Accepted: January 11, 2024
Published: January 19, 2024

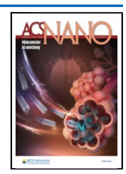

https://doi.org/10.1021/acsnano.3c09310
ACS Nano 2024, 18, 2685−2707

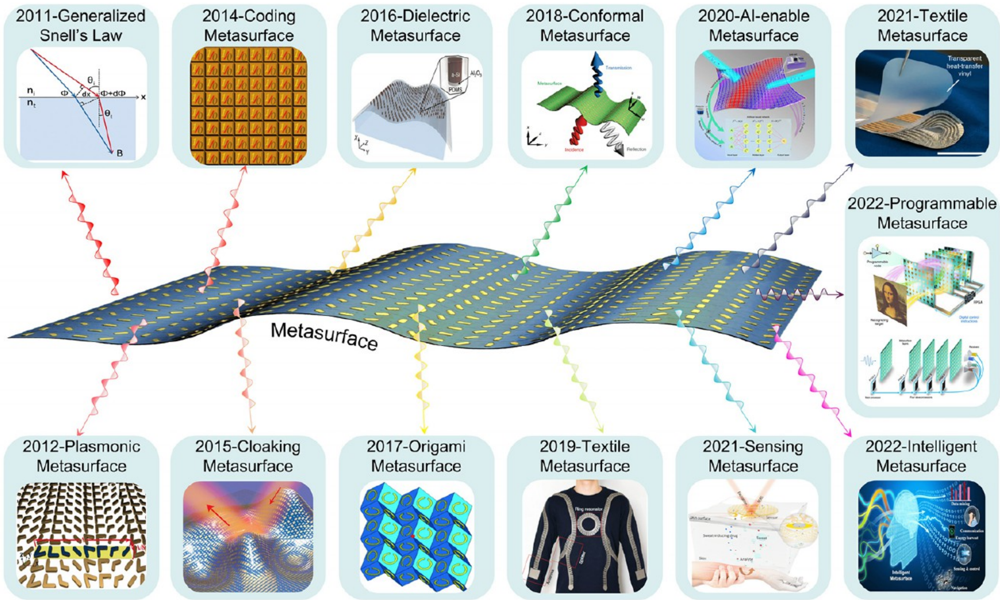

Figure 1. A brief chronology of the evolution of modern optical metasurfaces. 2011: Generalized Snell's law of refraction. Reproduced with permission.[99] Copyright 2011, AAAS. 2012: Plasmonic metasurface for nanoantenna interface. Reproduced with permission.[100] Copyright 2012, AAAS. 2014: Digitally coding metasurface. Reproduced with permission.[101] Copyright 2014, Springer Nature. 2015: Ultrathin cloaking metasurface. Reproduced with permission.[102] Copyright 2015, AAAS. 2016: Conformal dielectric metasurface. Adapted with permission under a Creative Commons CC BY license from ref 103. Copyright 2016, Springer Nature. 2017: Origami-based mechanically reconfigurable metasurface. Reproduced with permission.[104] Copyright 2017, Wiley-VCH. 2018: Different modeling methods for free-form conformal metasurface. Adapted with permission under a Creative Commons CC BY license from ref 105. Copyright 2018, Springer Nature. 2019: Textile-metasurface-based wireless body sensor network. Reproduced with permission.[88] Copyright 2019, Springer Nature. 2020: Deep-learning-enabled self-adaptive metasurface. Reproduced with permission.[106] Copyright 2020, Springer Nature. 2021: Epidermal sensing metasurface. Adapted with permission under a Creative Commons CC BY license from ref 86. Copyright 2021, AAAS. 2021: Textile-metasurface-based near-field multibody area network. Reproduced with permission.[89] Copyright 2021, Springer Nature. 2022: Deep-neural-network-based programmable metasurface. Reproduced with permission.[107] Copyright 2022, Springer Nature. 2022: Intelligent metasurfaces. Adapted with permission under a Creative Commons CC BY license from ref 93. Copyright 2022, Springer Nature.

mechanical, and thermal) not due to the chemical composition of materials but rather from their internally engineered structures. Unlike traditional materials, the concept of metasurfaces is versatile, encompassing a range of fields.[80−83] This includes optical,[80] elastic,[81] and acoustic metasurfaces,[82] which manipulate of electromagnetic, elastic, and acoustic waves, respectively. Recently, metasurfaces have captured increasing attention due to their advantages over 3D metamaterials, such as reduced losses, simplified design, and nanofabrication, and enhanced practicality.[80,84] Here, we mainly focus on optical metasurfaces. By using the subwavelength-sized meta-atoms artificially arranged at the 2D interface, optical metasurfaces based on either reflection or refraction can realize sufficient phase modulation without the long distance required for light propagation, thus leading to higher efficiency with much less attenuation. Therefore, at this stage, metasurfaces are better carriers for realizing amazing optical phenomena.

Conventional metasurfaces are mostly planar and rigid, which greatly limits their application since the world is curvaceous, complex, and dynamic. Such a mismatch has spurred many efforts toward flexible metasurfaces.[85−89] On the other hand, flexibility enables an additional dimension of possibility to control the light−matter interaction. During the past few years, this emerging field has experienced rapid development and advancement. There are many reviews from different perspectives,[80,84,90−94] but most of them focus on the interesting physical phenomena and academic merits. A state-of-the-art review from the perspective of versatile and innovative applications, together with deep insights about practical conformal challenges, is still highly desired to benefit the community. Certainly, the realization of the potential of flexible optical metasurfaces necessitates interdisciplinary research in areas such as optics, materials, and mechanics. The goal of this review is to arouse wide interest from different disciplines in the research of flexible optical metasurfaces. For this purpose, we start with a succinct overview of optical metasurfaces to show what they are and how they work, including the latest advances, underlying mechanisms, and basic classification. Then, several representative and advanced application scenarios are presented, followed by a summary of prevailing branches, to showcase what they can do. Special attention is given to the conformal challenges on complex curved surfaces to answer what we need to do at present. Finally, we close with an outline of the future directions and challenges of flexible optical metasurfaces.

2. RECENT ADVANCES OF OPTICAL METASURFACES

The research into optical metasurfaces has a storied history, but their real systematization and popularity occurred mainly in the past decade, after a breakthrough in theories, advanced materials, and modern micro/nanofabrication techniques.[95−98] Therefore, we will mainly discuss the progress since 2011. A brief chronology outlining some of the impressive milestones in this period is given in Figure 1. A pioneer work was reported in 2011, in which generalized laws of reflection and refraction that enable light propagation with phase discontinuities were

https://doi.org/10.1021/acsnano.3c09310
ACS Nano 2024, 18, 2685−2707

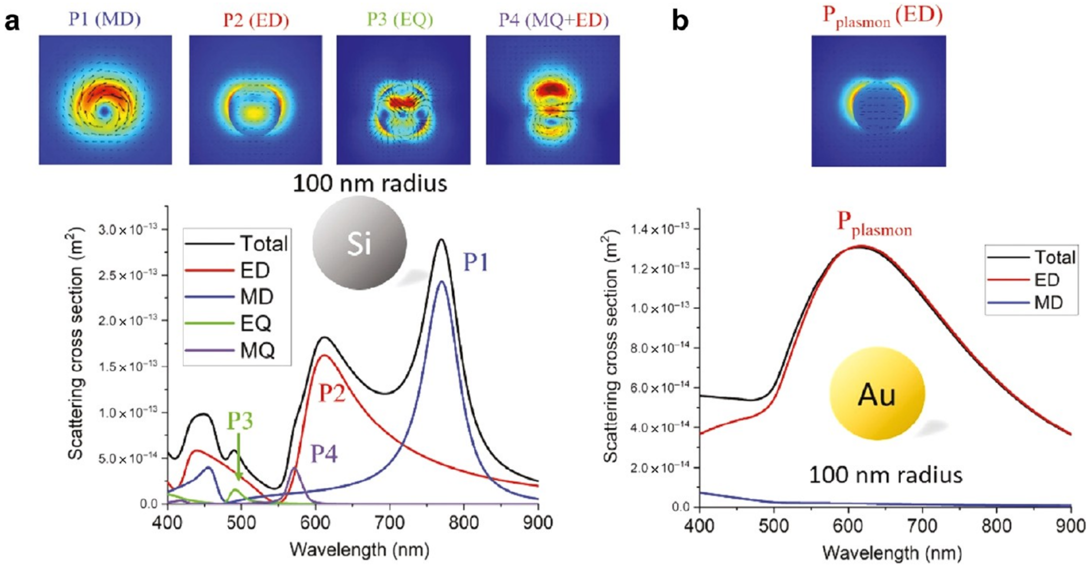

Figure 2. Different underlying mechanisms of optical metasurfaces. The multipole expansion of scattering spectra shows (a) in a 100 nm-radius Si nanosphere and (b) in a 100 nm-radius Au nanosphere. (a) In Mie resonances, the total radiation pattern is produced by electric dipole (ED), magnetic dipole (MD), electric quadrupole (EQ), and magnetic quadrupole (MQ) modes. The ED contribution shows the asymmetric pattern of a Fano resonance. (b) In plasmonic resonances, the total radiation pattern is dominated by ED. Adapted with permission under a Creative Commons CC BY license from ref 112. Copyright 2020, De Gruyter.

established.[99] Beyond the conventional counterparts which depend on gradual phase shifts accumulated during light propagation, phase discontinuities provide extra degrees of freedom and great flexibility in designing the bending of light beams over the scale of the wavelength. Before that, the phase change was limited by the optical properties of the materials, and an appreciable change often required a comparable or larger propagation length than the wavelength. Moreover, the properties still rely on the material parameters as they are governed by the conventional Snell's law. A plasmonic interface, consisting of an array of V-antennas, has been fabricated to confirm the generalized version of Snell's law. Subsequently, in 2012, Ni et al. extended such a plasmonic nanoantenna interface (∼30 nm) and presented wavefront control in a broadband wavelength range of 1.0 to 1.9 μm.[100] Thereafter, the breakthrough of basic principles ushered the research of optical metasurfaces into an emerging era. Many creative concepts, designs, and applications have been achieved, such as digitally coding metasurfaces,[101] ultrathin cloaking metasurfaces,[102] conformal dielectric metasurfaces,[103] mechanically reconfigurable metasurfaces,[104] modeling methods for free-form conformal metasurfaces,[105] textile-metasurface-based wireless body sensor network,[88] deep-learning-enabled self-adaptive metasurfaces,[106] wearable sensing metasurfaces,[86] textile-metasurface-based near-field multibody area network,[89] deep-neural-network-based programmable metasurfaces,[107] and intelligent metasurfaces.[93] It is foreseeable that optical metasurfaces will be one of the most dazzling unicorns in the scientific community.

3. FUNDAMENTALS OF OPTICAL METASURFACES

3.1. The Underlying Mechanisms of Optical Metasurfaces. The different underlying mechanisms of optical metasurfaces are shown in Figure 2, using the multipole expansion of scattering spectra (Figure 2a). This expansion can be observed in a 100 nm-radius silicon (Si) nanosphere and a 100 nm-radius gold (Au) nanosphere (Figure 2b). In plasmonic resonances, the total radiation pattern is dominated by the electric dipole (ED). However, in Mie resonances, the total radiation pattern is produced by the ED, magnetic dipole (MD), electric quadrupole (EQ), and magnetic quadrupole (MQ) modes. This difference exemplifies the fundamental distinction between the two, as metasurfaces' unparalleled control of light originates from the localized interaction between light and meta-atoms. Since surface-plasmon interaction is the most common approach to support subwavelength-sized localization of light, early metasurfaces are all plasmonic metasurfaces made of noble metallic nanostructures.[90] When exposed to an external electrical field, electrons of metallic particles are released from their equilibrium positions, and polarization occurs. Concomitantly, an internal depolarizing field for restoring the electrons is also aroused. When the external electrical field becomes time-harmonic, a collective oscillation with a phase shift of π over the spectral width of the resonance is induced. This phenomenon has led to a significant focus on plasmonic metasurfaces, resulting in many inspiring results.[86,108] However, some limitations are also obvious, such as being low-efficient due to high resistive loss, the high cost of noble metals, and incompatibility with current semiconductor processes.

Recently, to overcome the limitations of plasmonic metasurfaces, an alternative mechanism of light localization, known as Mie resonances,[109−112] has emerged to design optical metasurfaces. This method involves using purely high-index dielectric materials to substitute for noble metals. In contrast to the use of ohmic currents in plasmonic metasurfaces, the strong optical response in Mie resonances is offered by displacement currents, greatly reducing dissipative losses. Moreover, the displacement currents can support additional magnetic response, in contrast to the plasmonics with only electric response, resulting in a stronger total scattering efficiency. Besides, transparent dielectric materials often have advantages in reducing resistive loss and are compatible with the current semiconductor processes, etc.

https://doi.org/10.1021/acsnano.3c09310
ACS Nano 2024, 18, 2685−2707

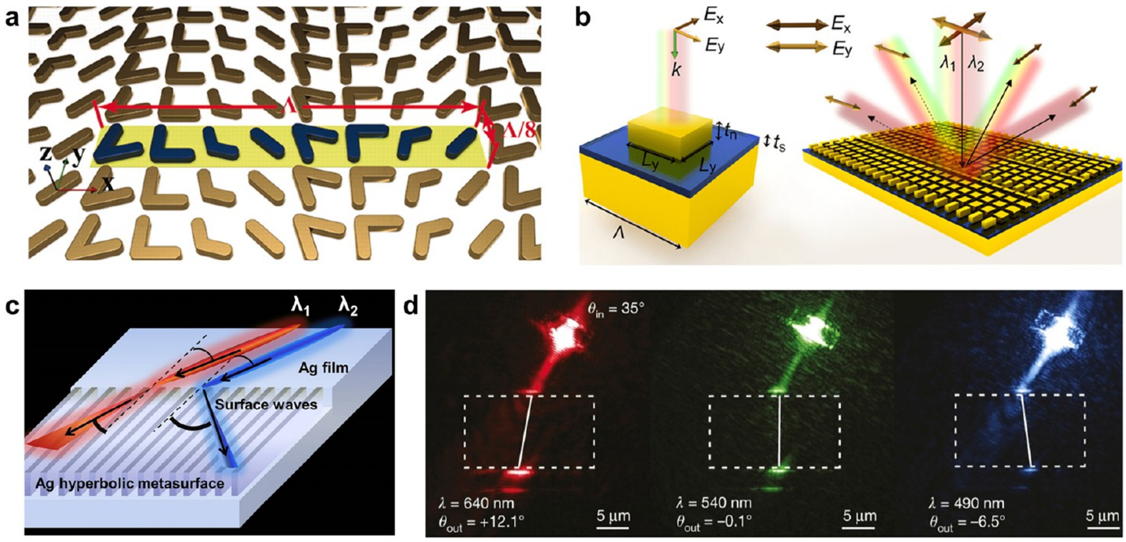

Figure 3. Plasmonic metasurfaces. (a) Multiresonance metasurface, a plasmonic nanoantenna array consisting of V-shaped gold antennas. (b) Gap-plasmon metasurface. A dual-band metasurface based on multiple gap-surface plasmon resonances. (c) Hyperbolic metasurface. (d) Visible-frequency hyperbolic metasurface. (c) Negative refraction of surface waves on the plane boundary of an Ag hyperbolic metasurface, and (d) it changes from normal refraction at λ = 640 nm to negative refraction at λ = 540 nm. (a) Reproduced with permission.[100] Copyright 2012, AAAS. (b) Reproduced with permission.[120] Copyright 2020, ACS. (c, d) Reproduced with permission.[121] Copyright 2015, Springer Nature.

Thus, dielectric metasurfaces are excellent complements to, and even potential replacements for, plasmonic metasurfaces. Nevertheless, considering that the stability of noble metals is not matched by the currently available dielectric materials, plasmonic metasurfaces are still of significance, especially for applications under complex conditions like aircraft stealth.[90,113,114]

Apart from plasmonic and Mie resonances, the asymmetric sharp Fano resonance is another mechanism to enable metasurfaces.[115] It is a coupled resonance that arises from the interference between broad nonresonant and narrow discrete resonant modes. Fano resonance is generally described as a physical phenomenon in a discrete localized state (weakly damping oscillator) that destructively interferes with a continuum of states (strongly damping oscillator), accompanying a π-phase shift at the resonance of discrete state (Lorentz oscillator model) and producing an asymmetrical spectral line shape.[112] Fano resonances can be observed both in plasmonic and dielectric systems, and the two main differences are as follows.[80] (i) Lower losses of dielectric particles allow Fano resonances in many geometries while plasmonic particles are often too large for Fano resonances due to metallic losses. (ii) Magnetic resonances of individual dielectric particles play a crucial role in Fano resonances. Therefore, Fano resonances show another possibility in high-efficiency, active, and nonlinear optical metasurfaces. On the other hand, thanks to the inherent interference between two or more resonances, Fano resonances are extremely sensitive to changes in geometry or local environment: slight perturbations can lead to dramatic shifts. This sensitivity makes Fano metasurfaces particularly attractive for chemical, molecular, and biological sensors.[116−118]

3.2. Classification of Optical Metasurfaces. In the above discussion, according to the underlying mechanisms, optical metasurfaces can be mainly divided into two categories: plasmonic and dielectric metasurfaces.[90] However, they only explained the different nucleation mechanisms of a π phase modulation. In fact, a 2π phase modulation is required to achieve full control of the wavefront. Thus, plasmonic and dielectric metasurfaces can be further classified into subcategories based on their physics for realizing a full 2π phase modulation. As of the current date, plasmonic metasurfaces mainly include multiresonance metasurfaces,[99,100] gap-plasmon metasurfaces,[119,120] hyperbolic metasurfaces,[121−123] etc. These metasurfaces typically work in reflective modes due to the low transmission efficiency of metals. Dielectric metasurfaces mainly include Huygens' metasurfaces,[124−126] high-contrast metasurfaces,[127,128] etc. In contrast, these metasurfaces rely on transmissive modes because of the high transmission of dielectric materials.

Multiresonance metasurfaces employ V-shaped nanoantennas to produce the phase modulation of $0-2\pi$ (Figure 3a).[100] The V-shaped nanoantennas can support two resonant modes: a symmetric mode and an antisymmetric mode. The superposition of these two resonance modes realizes the required phase coverage. Yet, the weak cross-polarization conversion and resultant low efficiency severely limit its application. Gap-plasmon metasurfaces use a metal−insulator−metal sandwich configuration, specifically a dielectric spacer sandwiched between a metallic array and metallic background, to obtain a 2π phase modulation. This spacer allows strong near-field coupling between the metallic components. Gap-plasmon metasurfaces have advantages in high efficiency and strong copolarization conversion but are limited to reflective applications.[119] Figure 3b shows a typical, albeit dual-band gap-plasmon metasurface using multiple gap-surface plasmon resonances.[120] Another important branch of plasmonic metasurfaces is hyperbolic metasurfaces. Within the hyperbolic regime, a metasurface exhibits metal-like properties in one direction and dielectric-like behaviors in the other, allowing the propagation of surface plasmon polaritons at the interface between them.[123] The significant benefits of hyperbolic metasurfaces include strong local field confinement and control of desired directions. The experimental demonstration of

https://doi.org/10.1021/acsnano.3c09310
ACS Nano 2024, 18, 2685−2707

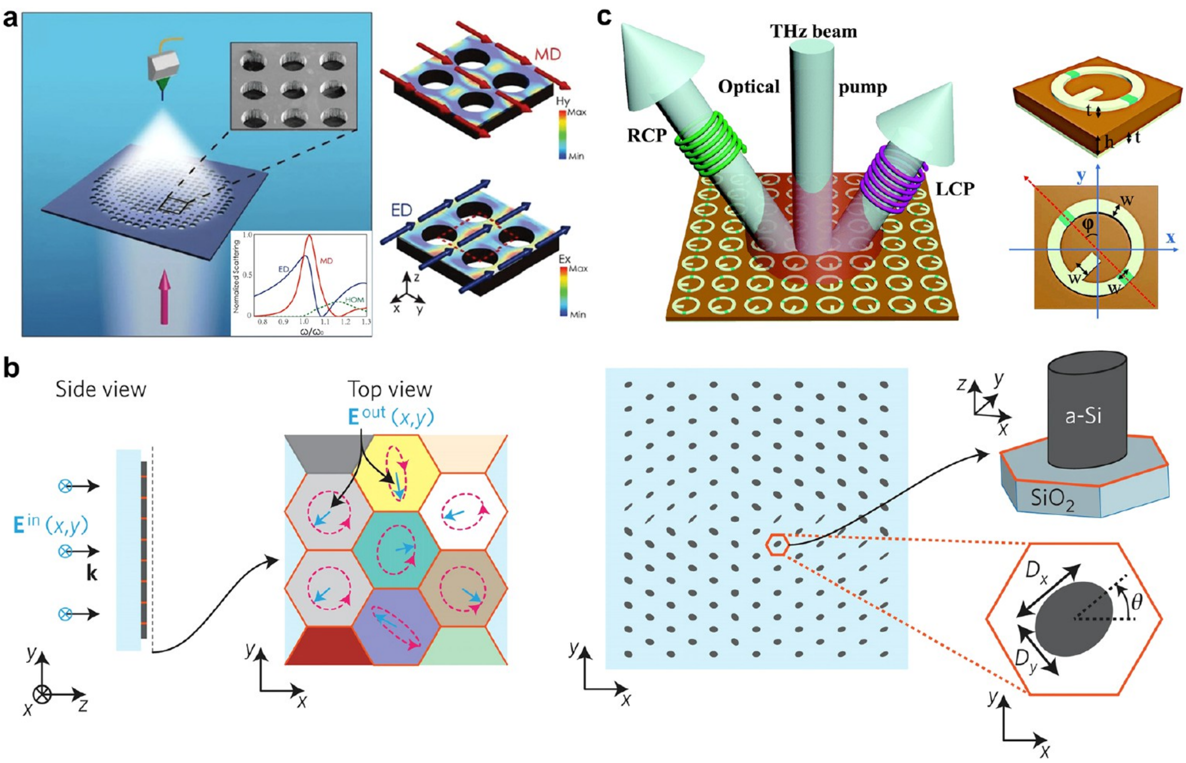

Figure 4. Dielectric metasurfaces. (a) Mie-Resonant membrane Huygens' metasurface. (b) High-contrast metasurface for complete control of phase and polarization. (c) 3-bit Pancharatnam−Berry coding metasurface and coding particles. (a) Reproduced with permission.[124] Copyright 2020, Wiley-VCH. (b) Reproduced with permission.[127] Copyright 2015, Springer Nature. (c) Reproduced with permission.[129] Copyright 2019, RSC.

hyperbolic metasurfaces was reported by High et al. in 2015, utilizing silver (Ag) grating nanostructures (Figure 3c).[121] The propagation direction of surface plasmons changes from normal refraction at λ = 640 nm to negative refraction at λ = 540 nm (Figure 3d).

Dielectric Huygens' metasurfaces, well-known dielectric metasurfaces, use the surface equivalence principle to realize a 2π phase modulation. Here, the spectrally overlapping electric and magnetic dipole resonances are orthogonal and comparable. This type of optical metasurface offers high transmission efficiencies in the microwave and near-infrared regimes but deteriorates rapidly at visible frequencies. Decker et al. experimentally demonstrated a high-efficiency dielectric Huygens' metasurface operating at near-IR frequencies in 2015.[124] Recently, Yang et al. introduced a concept of Mie-resonant membrane Huygens' metasurfaces (Figure 4a).[125] High-contrast metasurfaces, another type of dielectric metasurfaces,[128] allow quadrupoles and higher-order multipoles due to high refractive-index contrast. Unlike Huygens' metasurfaces dominated only by electric and magnetic dipole resonances, high-contrast metasurfaces with high refractive-index contrast enable quadrupoles and higher-order multipoles. The dielectric nanostructures in these metasurfaces act as truncated waveguides, thereby strongly confining light energy. High-contrast dielectric metasurfaces often exhibit superiority over their low-contrast counterparts in various aspects, such as improved efficiency, broadband performance, enhanced phase shifts, reduced scattering losses, and sharper resonances.[127,128] However, currently available high-contrast metasurfaces are mostly confined to limited materials. A seminal progress in high-contrast metasurfaces was conducted by Arbabi et al. in 2015 (Figure 4b),[127] where complete control of phase and polarization, with subwavelength spatial resolution and efficiency ranging from 72−97%, was achieved.

Pancharatnam−Berry metasurfaces, a special class of optical metasurfaces, exploit the Pancharatnam−Berry (PB) phase to achieve a 2π phase modulation.[84] The PB phase is a geometric phase that arises when a polarized light beam undergoes a cyclic evolution in its polarization state. This phase is associated with the geometric arrangement of the optical elements encountered by the light. With the nanoresonators rotating from 0° to 180°, the phase can be continuously modulated from 0 to 2π. The phase modulation is purely geometric and independent of dispersive resonance, and thus possesses a broad operational bandwidth. Moreover, due to the simple oriented replication of an identical nanoresonator, PB metasurfaces are both easy to design and have high tolerance. In the context of optical applications, PB metasurfaces are harnessed to design ultrathin devices capable of manipulating the polarization of incident light with high efficiency. Figure 4c shows a representative 3-bit Pancharatnam−Berry coding metasurface.[129] So far, the fundamentals of optical metasurfaces have been briefly presented. In the following section, we introduce various metasurface-based advanced applications.

4. ADVANCED APPLICATIONS OF OPTICAL METASURFACES

4.1. Imaging. Optical metasurfaces have found widespread use in the field of imaging, such as chiral imaging, super-resolution imaging, and computational intelligent imaging. Notable contributions include Khorasaninejad et al.'s work on compact and multispectral chiral imaging, which can simultaneously form two images with opposite helicity of an

https://doi.org/10.1021/acsnano.3c09310
ACS Nano 2024, 18, 2685−2707

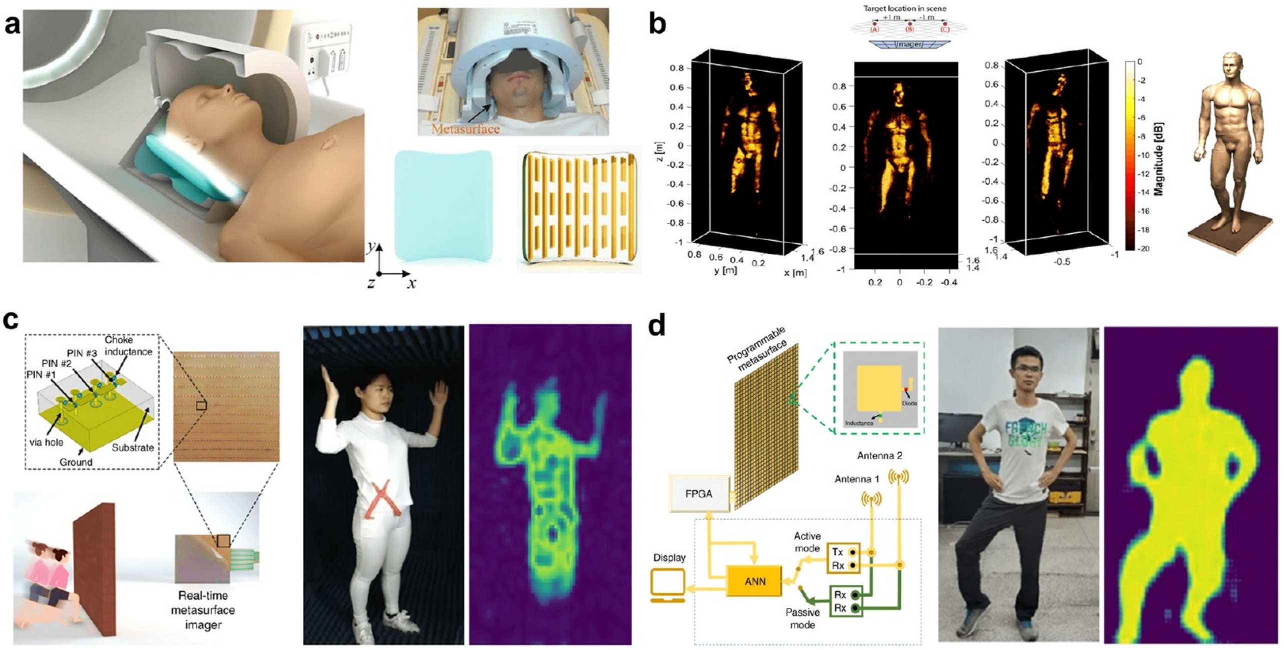

Figure 5. Metasurfaces-based bioimaging. (a) Metasurface-based ultrahigh field *in vivo* magnetic resonance imaging. (b) Metasurface-based least-squares image reconstruction of a mannequin. (c) Machine-learning-enabled metasurface-based reprogrammable imager for human body imaging. (d) *In situ* imaging results using the intelligent metasurface with an active microwave. (a) Adapted with permission under a Creative Commons CC BY license from ref 138. Copyright 2017, Springer Nature. (b) Adapted with permission under a Creative Commons CC BY license from ref 139. Copyright 2017, Springer Nature. (c) Adapted with permission under a Creative Commons CC BY license from ref 141. Copyright 2019, Springer Nature. (d) Adapted with permission under a Creative Commons CC BY license from ref 140. Copyright 2019, Springer Nature.

object within the same field-of-view.[130] Li et al. leveraged metasurfaces' nearly dispersionless feature of phase modulations to achieve broadband super-resolution imaging.[131] Zheng et al. demonstrated metasurface-based computational imaging encryption, utilizing a dual-channel Malus metasurface to encode different target images,[132] following the principle of single-pixel imaging. Moreover, optical metasurfaces have been seamlessly integrated into current optical systems, including two-photon microscopes, confocal microscopes, and optical coherence tomography (OCT) systems. Arbabi et al. experimentally demonstrated a compact two-photon microscope using a thin double-wavelength metasurface lens, with comparable performance to current systems based on graded-index lenses.[133] Chen et al. presented a metasurface-integrated confocal microscope with improved imaging capabilities, achieving an imaging spatial resolution of approximately 200 nm.[134] Additionally, Pahlevaninezhad et al. reported a metalens-implemented OCT system capable of obtaining clear and high-quality endoscopic imaging *in vivo* and *ex vivo*.[135]

Bioimaging stands out as a prominent area where optical metasurfaces have found wide applications and commercialization as fluorescence imaging or noninvasive bioimaging tools for diagnosis and observation. One early example is the enhancement of magnetic resonance imaging (MRI) with metasurfaces. Placing a metasurface consisting of an array of 14 × 2 wires inside the MRI scanner increases the RF magnetic field and the signal-to-noise ratio (SNR) locally, thereby improving the MRI scanning efficiency. The SNR shows a 2-fold increase over the case without the metasurface.[136] Shchelokova et al. also achieved similar SNR enhancement, showing a 3.3-fold increase for *in vivo* imaging at 1.5 T.[137] Additionally, to adapt to the curved profile of the human body, flexible and compact optical metasurfaces have been developed, as shown in Figure 5a, enabling in vivo human brain imaging in an ultrahigh commercial 7 T MRI system.[138] Moving toward more advanced applications, active biosensing with intelligent metasurfaces has emerged. Gollub et al. employed a frequency-diverse metasurface, comprising 24 transmit and 72 receive panels, to realize computational imaging and enable human-scale scene reconstruction and security checks (Figure 5b).[139] In 2019, Cui's group pioneered the concept and implementation of intelligent metasurface imagers.[140,141] Figure 5c and 5d illustrate the machine-learning reprogrammable metasurface imager[140] and deep-learning programmable metasurface imager and recognizer,[141] respectively. The former imager, after training, produces real-time high-quality imaging and high-accuracy object recognition directly from the imager, without the need for time-consuming image reconstruction (Figure 5c). The latter imager enables remote, economical, and instantaneous *in situ* full-scene imaging and adaptive recognition of complicated human behaviors (Figure 5d). These notable demonstrations confirm that optical metasurfaces have evolved into an emerging and powerful platform for imaging.

4.2. Biosensing.

Recently, optical-metasurface-based healthcare has drawn a lot of attention, owing to its distinct capability to control electromagnetic fields in the vicinity of the human body.[87] This innovative approach provides compelling potential for healthcare monitoring compared to conventional bioelectronic interfaces. Figure 6a gives a schematic illustration of the fundamental mechanism underlying light-based biosensing,[142] which involves detecting modified (absorbed and scattered) photons after photophysical interaction to

https://doi.org/10.1021/acsnano.3c09310
ACS Nano 2024, 18, 2685−2707

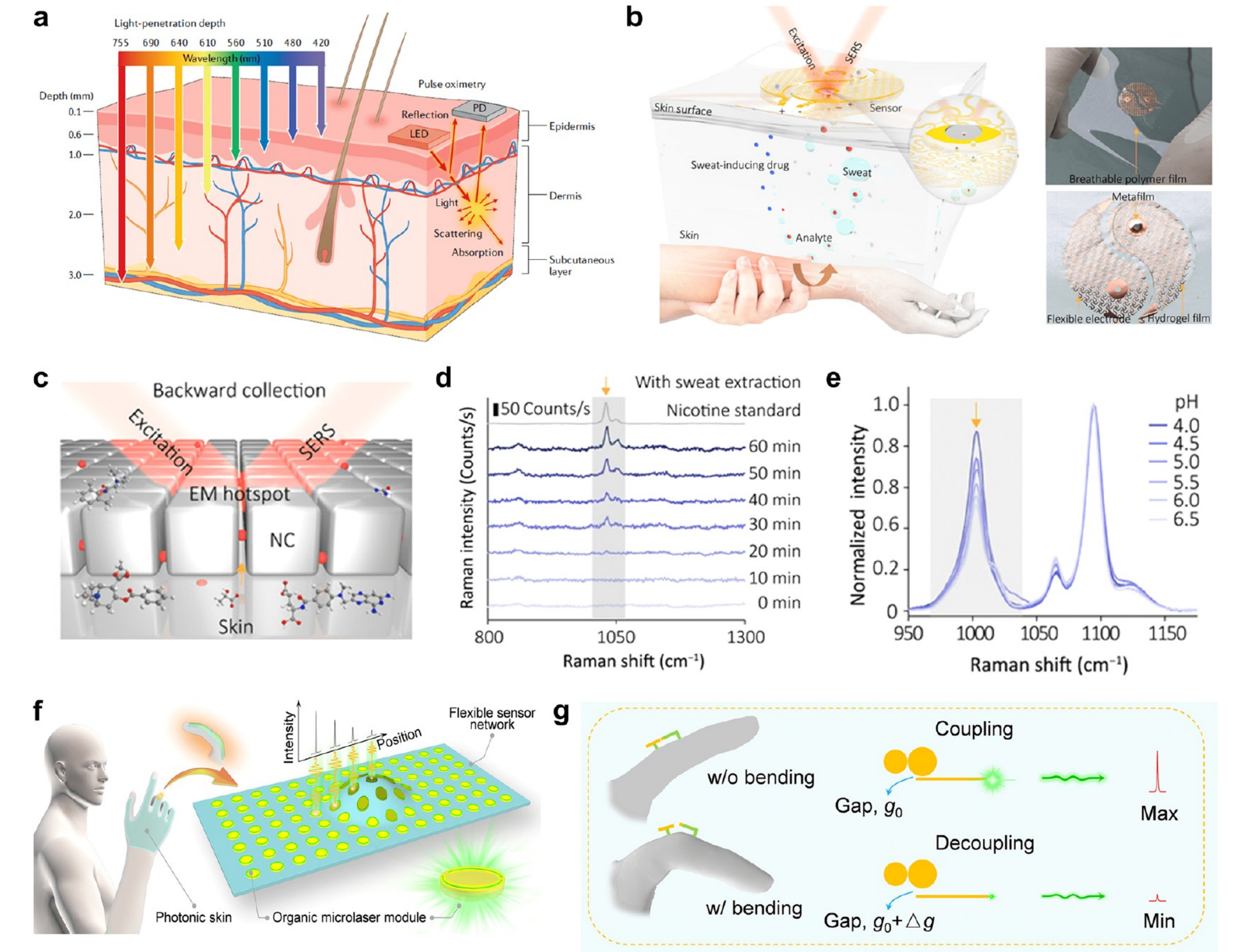

Figure 6. Metasurface-based biosensing. (a) Schematic of the fundamental mechanism underlying light-based biosensing. (b) Wearable plasmonic-metasurface sensor for noninvasive molecular sensitivity. (c) SERS sensing principle of an ordered silver nanocube metafilm. (d) Nicotine detection on human skin using a wearable plasmonic-metasurface sensor with sweat extraction. (e) SERS responses of the sensor in different buffers (pH 4.0−6.5). (f) Concept of artificial photonic skin system based on organic microlaser array. (g) Working principle of flexible mechanical sensors for gesture recognition. (a) Reproduced with permission.[142] Copyright 2020, Springer Nature. (b, c, d, e) Adapted with permission under a Creative Commons CC BY license from ref 86. Copyright 2021, AAAS. (f, g) Adapted with permission under a Creative Commons CC BY license from ref 145. Copyright 2021, AAAS.

obtain biometric information from biological tissues. In compared to conventional electrical biosensing mechanisms, light-based biosensing can overcome the drawbacks of signal hysteresis, power consumption, and electromagnetic interference. Metasurface-based sensing, in essence, is a resonance sensing mechanism that converts the target signals into electromagnetic resonance responses. This process involves quantifying the variation of the local electromagnetic field distribution, typically characterized by resonance frequency. For example, the pulse can be remotely collected and demodulated by the shift and intensity change of resonance frequency through the metasurface-based wireless and passive biosensing mechanism.[98] The metasurface-based approach offers various advantages, including high sensitivity due to the strong local confinement of electromagnetic fields, wide range achieved by free manipulation of wavefront phase, amplitude, and polarization, high efficiency through the control of desired directions, high accuracy by enhancing light−matter interactions at the deep subwavelength scale, large capacity for multiplexing, real-time and *in situ* detection, and wireless, passive, noninvasive, and anti-interference features. All these salient traits make metasurface-based biosensing a thought-provoking and groundbreaking approach to overcome the limitations of current bioelectronic interfaces.

Following the successes of electronic skin during the past two decades, the concept of photonic skin that can be directly mounted onto the skin is an important direction for metasurface-based healthcare applications. In contrast to its electronic analog with complex electrical components and interconnection, photonic skin realizes wireless communication with an ultrafast data exchange rate and provides real-time feedback on healthcare status. The unit cell of optical metasurface reminisces about resonant wireless biosensors. Before metasurface-based biosensing, passive arrays of resonant biosensors have been used for continuous, wireless, and real-time pressure monitoring and mapping inside the body, as well as *in vivo* intracranial pressure in proof-of-concept mice studies.[143] A multifunctional array of hydrogel-interlayer

https://doi.org/10.1021/acsnano.3c09310
ACS Nano 2024, 18, 2685−2707

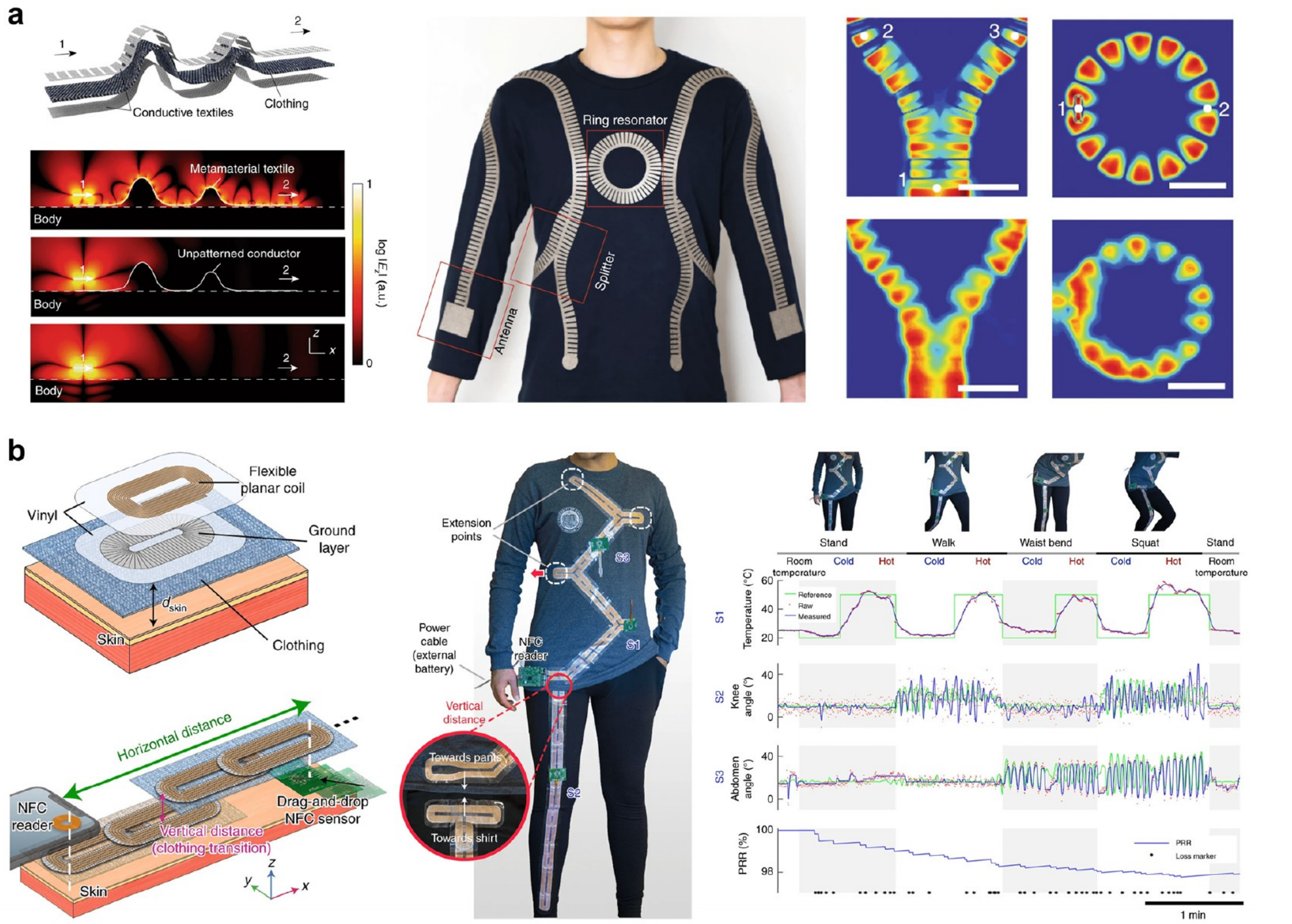

Figure 7. Metasurface-textile-based wireless body sensor network. (a) Metasurface textile network integrating splitters, antennas, and a ring resonator. (b) Metasurface-textile-based near-field multibody area networks, enabling long-distance near-field communication-based magneto-inductive waves along and between multiple objects. (a) Reproduced with permission.[88] Copyright 2019, Springer Nature. (b) Reproduced with permission.[89] Copyright 2021, Springer Nature.

resonant biosensors has also been used to wirelessly and passively monitor pressure, sweat, and temperature simultaneously by radio frequency or near-field communication.[144] Recently, Wang et al. proposed an interesting plasmonic-metasurface sensor capable of noninvasive and universal molecular recognition ability inside the body (Figure 6b).[86] Plasmonic metasurface with surface-enhanced Raman scattering (SERS) was introduced to solve the challenge of tracking multiple internal analytes simultaneously (Figure 6c). Real-time monitoring of nicotine (Figure 6d) and different buffers (Figure 6e) verified the effectiveness. Afterward, Zhang et al. presented a photonic skin based on flexible organic microlaser arrays (Figure 6f).[145] The outcoupling of organic microcavity lasers depends on substrate deformation, and the 2D array of these mechanical sensors on a flexible chip enables spatially resolved detection of local deformations like gesture recognition (Figure 6g). Although it is not strictly a metasurface-based photonic skin, such photonic skin has high scalability for further metasurface-based functionality expansions due to the same light-based biosensing mechanism and 2D arrayed form.

Metasurface-based wireless body sensor network that can be integrated into clothing is another significant achievement. Its advantages are mainly reflected in the following aspects. First, metasurface-based textiles are contactless to the body and can circumvent the challenges of breathability, conformability, comfortability, replacement, and so on. Second, current wireless communications typically rely on radio frequency techniques that result in bulky and energy-consuming systems, but subwavelength metasurfaces can overcome these limitations. Third, the human body is a lossy, heterogeneous, and dispersive medium, and metasurfaces can enhance the light—matter interaction. Fourth, the human body is dynamic, and its demand greatly varies between individuals, so metasurfaces can be customized. Fifth, in contrast to conventional radiative approaches, metasurface-based localized surface transmissions can greatly improve efficiency, security, and anti-interference. In 2019, Tian et al. realized a fascinating wireless body sensor network based on metasurface-based textiles (Figure 7a).[88] Instead of typical radiative radio-wave communications, a special surface-plasmon-like communication around the metasurface-based textiles was used to obtain more energy-efficient and secure performance. The transmission efficiency can be increased by over 3 orders of magnitude (>30 dB), and the wireless communication can be localized within 10 cm of the body. After that, in 2021, Hajiaghajani et al. reported a near-field multibody area network by metasurface-based textiles (Figure 7b).[89] Flexible anisotropic magneto-inductive elements composed of discrete, planar, and flexible micro-electronics-free loops were used to empower tunability,

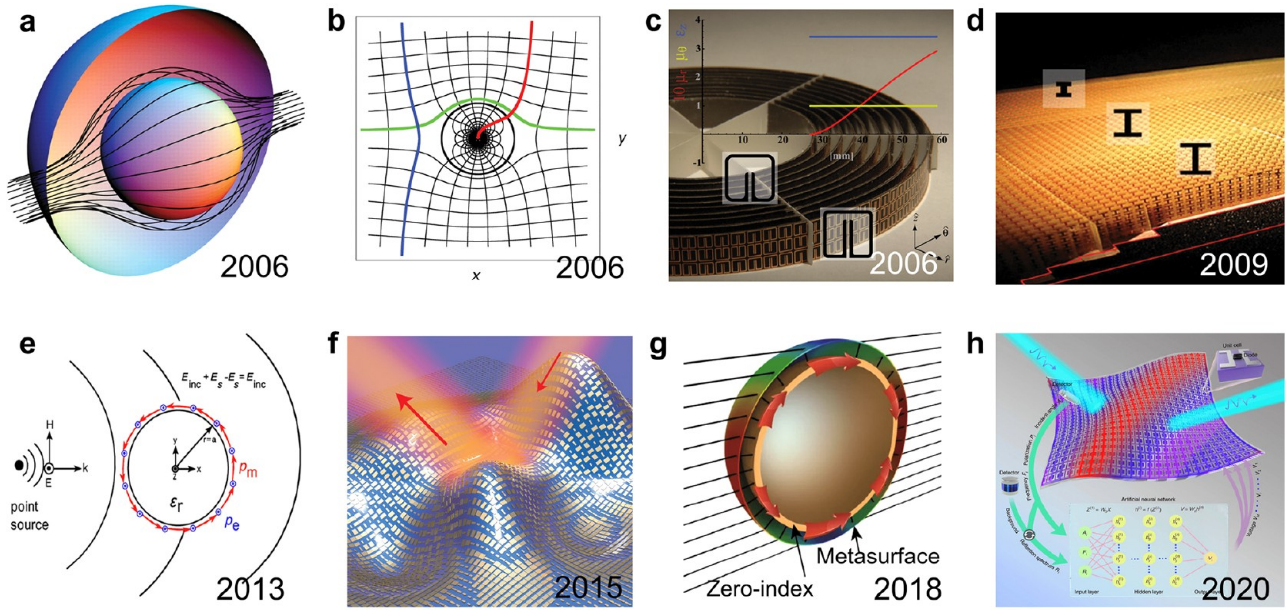

Figure 8. Metasurfaces-based electromagnetic cloaking. (a) Transformation optics. (b) Optical conformal mapping. (c) First practical realization of metamaterial electromagnetic cloak. (d) Experimental realization of 3D carpet cloak. (e) Active electromagnetic cloak. (f) Ultrathin metasurface-based optical cloak. (g) Hybrid invisibility cloak based on the integration of transparent metasurfaces and zero-index materials. (h) Deep-learning-enabled metasurface-based self-adaptive cloak. (a) Reproduced with permission.[146] Copyright 2006, AAAS. (b) Reproduced with permission.[147] Copyright 2006, AAAS. (c) Reproduced with permission.[148] Copyright 2006, AAAS. (d) Reproduced with permission.[150] Copyright 2009, AAAS. (e) Reproduced with permission under a Creative Commons Attribution 3.0 License from ref 152. Copyright 2013, American Physical Society. (f) Reproduced with permission.[102] Copyright 2015, AAAS. (g) Adapted with permission under a Creative Commons CC BY license from ref 153. Copyright 2018, Springer Nature. (h) Reproduced with permission.[106] Copyright 2020, Springer Nature.

compatibility, and expansibility. The plug-and-play ability of near-field communications enables pick-and-place features that allow wireless sensing nodes to be switched at will.

4.3. Cloaking. Arguably, cloaking represents one of the most captivating and promising applications of optical metasurfaces. The concept of an invisibility cloak has fascinated humanity for millennia, but remained a dream until the advent of metamaterials that can reconstruct the scattering field of a targeted object. The modern invisibility cloak traces its origins to 2006, when Pendry et al.[146] and Leonhardt[147] independently proposed the fundamental theories of transformation optics (Figure 8a) and optical conformal mapping (Figure 8b), respectively. Transformation optics establish a relationship between space geometry and inhomogeneous media via coordinate transformation, creating a mathematical or geometric framework for controlling electromagnetic waves at will. The underlying mechanism rests on the form-invariance of Maxwell's equations under coordinate transformations. Conversely, optical conformal mapping provides a generalized methodology for designing media that can achieve perfect invisibility within the precision of geometrical optics. These seminal works heralded an emerging era in cloaking, leading to abundant research about metamaterials-based cloaking. Schurig et al. presented the practical realization of such a cloak,[148] specifically, a 2D cylindrical cloak made of split-ring resonators at microwave frequencies (Figure 8c). The experimental performance, however, was hampered by the cloak's bulky, inhomogeneous, and anisotropic compositions. In response, extensive efforts have been undertaken to overcome these limitations, including innovations such as quasi-conformal mapping,[149] broadband ground-plane cloak (Figure 8d),[150] 3D carpet cloak,[151] and active cloak (Figure 8e),[152] among others.

Another significant advancement in the field of optical metasurfaces occurred in 2015 when Ni et al. developed an ultrathin metasurface-based optical cloak (Figure 8f).[102] This 80 nm thick cloak, in contrast to its bulkier predecessors, removed the constraint of conformability on curved surfaces. Subsequent research in cloaking has become increasingly practical due to the intrinsic advantages of metasurfaces. In 2016, the concept of conformal metasurfaces was employed to uncouple the geometric shape and optical properties of arbitrary objects.[103] Metasurface-based cloaks, however, are limited to reflection geometry. To address this issue, a hybrid cloak functioning in transmission geometry was proposed by incorporating transparent metasurfaces and zero-index materials (Figure 8g).[153] Recent innovations include a deep-learning-enabled self-adaptive metasurface cloak (Figure 8h),[106] and applications in various fields like acoustics,[154] elastodynamics,[155] electrics,[156] hydrodynamics,[157] mechanics,[158,159] thermodynamics,[160] etc. Although electromagnetic cloaks have become more tangible with the development of optical metasurfaces in the past decade, and many milestones have been reached, they are yet to evolve into practical applications. Addressing this challenge requires comprehensive and interdisciplinary expertise.

4.4. Multifunction. As the study of optical metasurfaces continues to evolve, multifunctionality has emerged as another crucial trend. The integration of diverse functions can significantly enhance adaptability to complex environments and broaden application scopes.[161−164] Figure 9 illustrates a multifunctional smart skin for next-generation aircraft, incorporating optical sensing and location, electromagnetic

https://doi.org/10.1021/acsnano.3c09310
ACS Nano 2024, 18, 2685−2707

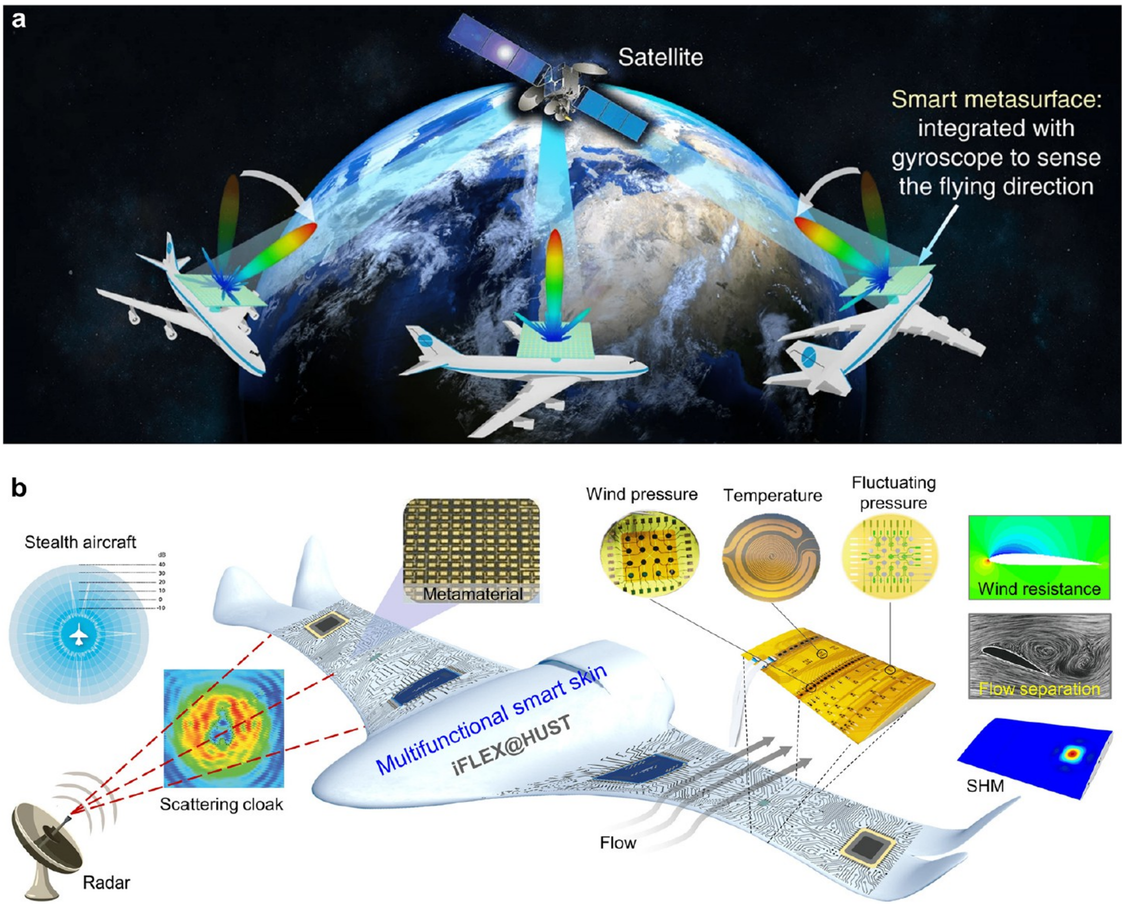

Figure 9. Multifunctional smart skin. (a) Smart metasurface integrated with gyroscope to sense the flying direction. (b) Schematic of next-generation iFlexSense that processes dual excellent sensitivity of aerodynamic parameters and stealth ability. (a) Adapted with permission under a Creative Commons CC BY license from ref 114. Copyright 2019, Springer Nature. (b) Reproduced with permission.[98] Copyright 2022, Wiley-VCH.

cloaking, and aerodynamical sensing. In one application (Figure 9a), motion-sensitive metasurfaces coupled with a three-axis gyroscope can sense and adjust flying direction.[114] In another example (Figure 9b), the integration of cloaking with aerodynamic sensing can greatly increase survivability and maneuverability for future aircraft. Stealth capability that can greatly increase survivability is the definite trend of future aircraft. Meanwhile, unmanned aerial vehicles that can alter the aerodynamic shape according to different flight environments and missions are another inevitable direction. In virtue of the *in situ* measurement of aerodynamical parameters (e.g., wind pressure, fluctuating pressure, temperature, and stress), automated systems will be able to rapidly exploit tactical opportunities consistent with operational direction, significantly enhancing maneuverability and sustainability.[63] Thus, electromagnetic cloaking and aerodynamical sensing supplement and improve each other, which can boost the development of the next-generation aircraft collectively.

Moreover, similar functions based on different mechanisms can cross-verify, enhancing system robustness. The combination of different sensing technologies, like optical and electronic sensors, creates synergies and reduces potential failures. Also, high integration streamlines space, weight, power consumption, and redundancy, promoting efficiency. Finally, the merging of optical metasurfaces and flexible electronics, facilitated by approaches like the field-programmable gate array (FPGA), introduces a fresh perspective on "smart skin" with extensive implications for future development.[98]

5. IMPORTANT TRENDS OF OPTICAL METASURFACES

5.1. Mechanically Reconfigurable Metasurfaces. Reconfigurable metasurfaces offer dynamic control over optical properties and have become a vital research focus. These metasurfaces enable the switching between configurations and induce variations of functions. It should be made clear that the terms "reconfigurable", "programmable", "coding", "digital", and other similar words are often used interchangeably in the literature about metasurfaces, but in fact, they have different meanings. Within this work, we distinguish them as follows: (i) reconfigurable metasurfaces that involve mechanical deformation and (ii) programmable/coding/digital metasurfaces that are specifically modulated by external stimuli (i.e., circuit and light). Generally, strategies to achieve reconfigurable metasurfaces can be classified into three approaches: (a) stretchable materials like polydimethylsiloxane (PDMS) and Ecoflex,[165] (b) liquid metals,[166−169] and (c) origami-based,[170] and kirigami-based flexible mechanical metamaterials.[171] These strategies hinge on precisely linking varying optical properties with mechanical deformations. Each approach offers extra possibilities and applications such as tunable lenses, resonators, and reconfigurable 2D-to-3D structures.

https://doi.org/10.1021/acsnano.3c09310
ACS Nano 2024, 18, 2685−2707

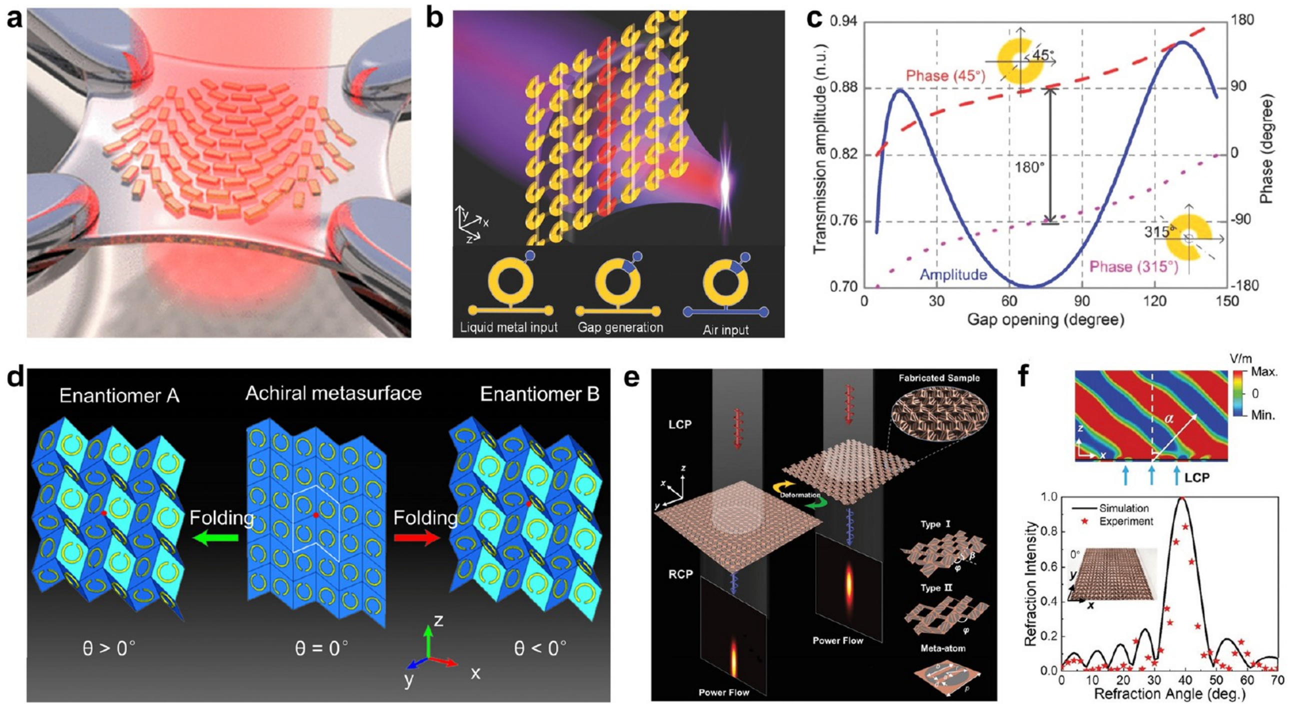

Figure 10. Mechanically reconfigurable metasurfaces. (a) Mechanically reconfigurable metasurface based on intrinsically stretchable materials: tunable metasurface and flat optical zoom lens on a stretchable substrate. (b) Mechanically reconfigurable metasurface based on liquid metals: flat lens with tunable phase gradient by using liquid metals. (c) Transmission amplitude and phase as functions of the gap openings and orientations of the unit cell. (d) Mechanically reconfigurable metasurface based on origami designs: origami-based reconfigurable metamaterials for tunable chirality. (e) Mechanically reconfigurable metasurface based on kirigami designs: kirigami-inspired reconfigurable metalens. (f) E-field amplitude profiles of the transmitted wave and far-field results. (a) Reproduced with permission.[165] Copyright 2016, ACS. (b, c) Reproduced with permission.[166] Copyright 2015, Wiley-VCH. (d) Reproduced with permission.[170] Copyright 2017, Wiley-VCH. (e, f) Reproduced with permission.[171] Copyright 2022, Wiley-VCH.

In the first strategy, reconfigurable metasurfaces are deployed on stretchable substrates. Upon stretching the substrate, the lattice changes, allowing continuous tuning of the wavefront. For example, Ee and Agarwal proposed such a metasurface with an array of gold (Au) nanorods embedded in a thin stretchable PDMS film,[165] showing tunable optics at the visible frequency (Figure 10a). Moreover, an ultrathin flat zoom lens was developed as a practical application, whose focal length can be changed by stretching the substrate. The second strategy involves liquid metals patterned and encapsulated into earmarked channels. The liquid metals can be injected into the microchannels and filled in the channels with controlled pressure similar to pneumatic valves. This allows for an array of such independently tunable elements, forming the mechanism to build reconfigurable metasurfaces. The resonant electromagnetic properties can be tailored at will by dynamically changing the filling factor of the resonators. As a paradigm, Zhu et al. presented a flat lens with a tunable phase gradient using a liquid metal-based reconfigurable metasurface (Figure 10b).[166] Figure 10c shows the transmission amplitude and phase as the functions of the gap openings and orientations of the unit cell. The third strategy employs popular kirigami-based and origami-based flexible mechanical metamaterials. This approach greatly enriches the structural designs with features like programmable morphability and configurable/reconfigurable 2D-to-3D transformability. Noteworthily, although kirigami and origami share many things in common such as strain-isolated tessellation, kirigami is more about auxetic stretchability based on negative Poisson's ratio (NPR) while origami is more about spatial freedom and reconfigurability based on dynamically deterministic foldability. The NPR can greatly improve the biaxial stretchability and then significantly reduce the stress–concentration. The reconfigurability allows the switch of different configurations and different functionality. One of the underlying principles of kirigami and origami is that local large but low-energy deformations render the collective shape-shifting transformations. The debut of origami-based reconfigurable metasurface appeared in 2017 (Figure 10d),[170] with the capability to switch electromagnetic responses between chiral and nonchiral states. Recently, a kirigami-based reconfigurable gradient metasurface was developed (Figure 10e).[171] This 2D metasurface can be continuously transformed into 3D structures, allowing for tunable optical properties (Figure 10f). As a proof-of-concept, two meta-devices including a reconfigurable metalens and switchable anomalous refractor were experimentally verified.

5.2. Digitally Coding Metasurfaces. The concept of coding metasurfaces emerged with the work of Cui et al. in 2014 (Figure 11a).[101] These metasurfaces were composed of only two types of unit cells, namely “0” and “1” cells, with 0 and π phase responses. The switch between “0” and “1” was controlled via a biased diode. Moreover, the 1-bit coding can be extended to 2-bit coding or higher. This includes the “00”, “01”, “10”, and “11” cells corresponding to the phase responses of 0, $\pi/2$, π, and $3\pi/2$, respectively. By coding the binary system with an FPGA, digital control of different functionalities can be realized, enabling a single coding metasurface to possess multiple functions. This epoch-making work established a link between metasurface physics and digital information science. Since then, the Cui group has achieved

https://doi.org/10.1021/acsnano.3c09310
ACS Nano 2024, 18, 2685−2707

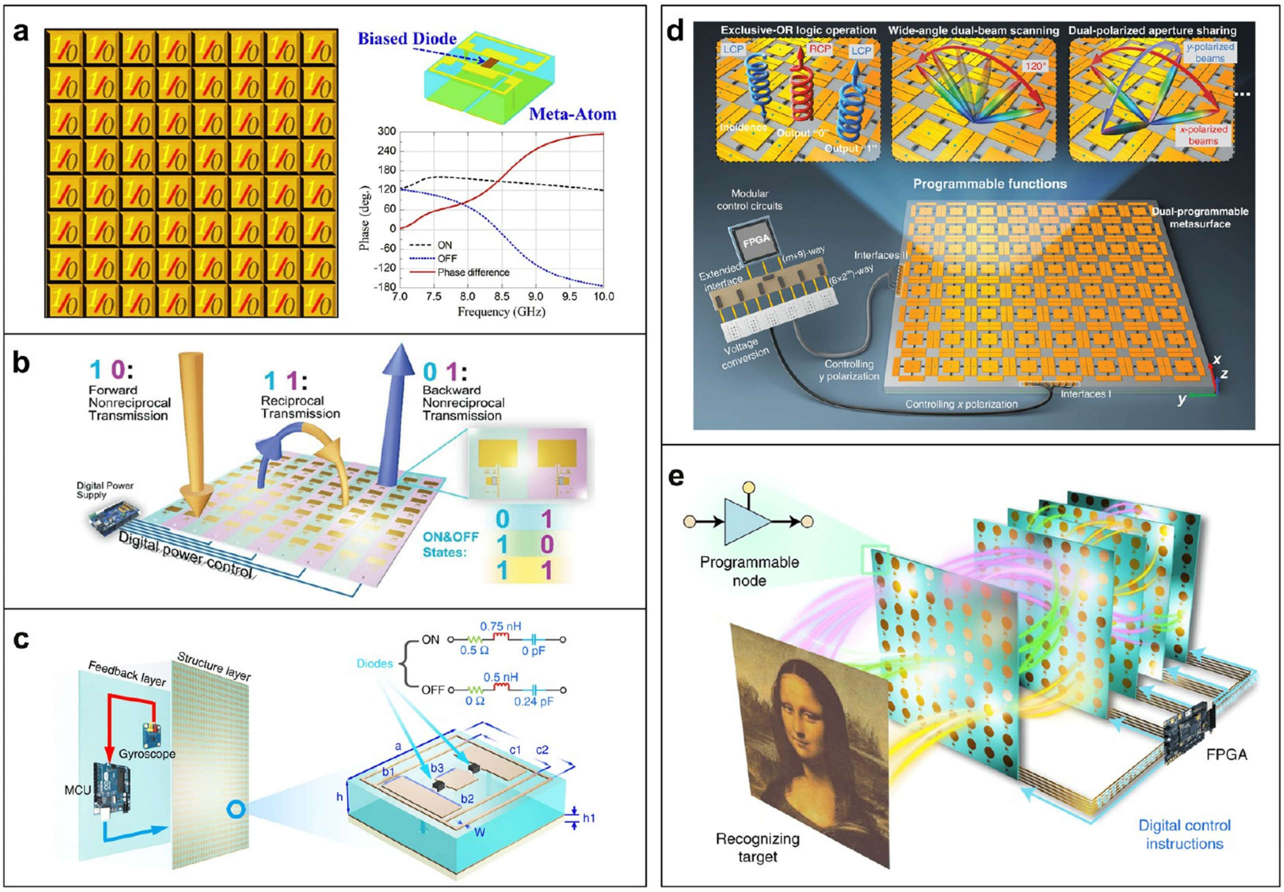

Figure 11. Digitally coding metasurfaces. (a) Pioneer FPGA-controlled coding metasurface. (b) Coding nonreciprocal metasurface. (c) Self-adaptive coding metasurface. (d) Polarization-controlled dual-coding metasurface. (e) Deep-neural-network-based coding metasurface. (a) Reproduced with permission.[101] Copyright 2014, Springer Nature. (b) Reproduced with permission.[176] Copyright 2019, Wiley-VCH. (c) Adapted with permission under a Creative Commons Attribution 4.0 International License from ref 114. Copyright 2019, Springer Nature. (d) Adapted with permission under a Creative Commons CC BY license from ref 186. Copyright 2020, Wiley-VCH. (e) Reproduced with permission.[107] Copyright 2022, Springer Nature.

many fantastic accomplishments in this direction, ushering in an emerging era of light manipulation. The theoretical progress includes diffuse scattering,[172] addition theorem,[173] nonlinearity,[174] nonreciprocity (Figure 11b),[175,176] and so on. The encoding approach has evolved from initial 1-bit to 2-bit (Figure 11c),[101,114] then to 3-bit,[177] multibit,[178] deep learning algorithms,[179] deep neural networks,[107] and even recent mind control via brainwaves.[180] Various controlled methods have been introduced, such as spatial coding,[181] time-domain coding,[182] frequency coding,[183] space-time-coding,[184] and space-time-frequency coding.[185]

In addition, the objects have been expanded to allow independent modulation of phases, amplitudes, and polarizations (Figure 11d),[186] and to control both amplitude and phase[187] and both phase and polarization.[188] Many interesting applications have been presented including antenna,[189] hologram,[190] Doppler,[191] and DC remote cloak,[192] analog signal processing,[193] topological insulators,[194] wireless communication,[195] wireless recognition for prosthesis,[196] image recognition (Figure 11e),[107] and wireless power transfer.[197] Moreover, innovative functional materials such as liquid metals[198] and piezoelectronics[199] have been integrated into the coding metasurfaces. Since the research of coding metasurfaces has become popular, numerous reviews provide in-depth discussions on specific topics. Readers interested in exploring more details may refer to other reviews.[93,200−204] Interestingly, besides the optics, the concept of coding metasurfaces can also be applied to elastic and acoustic metasurfaces, areas ripe for exploration. However, the currently available coding metasurfaces are planar and rigid, which greatly impedes their applications since the world is curved and dynamic, consisting of various arbitrary surfaces. How to realize conformal coding metasurfaces that can manipulate optical properties on complex surfaces is the emphasis and difficulty in the next research. The challenges to be faced include but are not limited to the conformal design of arrayed patterns, conformal fabrication, conformal circuit design and digital control, conformal integration of numerous control units, and so on. The shift from 2D to 3D coding metasurfaces is an inevitable trajectory, but its true commencement is still on the horizon.

5.3. Conformal Metasurfaces. To transcend the limitations of flat and rigid structures, there is a strong demand for conformal metasurfaces capable of operating with arbitrarily curved shapes. Currently, the solutions to this challenging issue can be classified into four categories: (i) flexible substrates, (ii) multiplane approximations, (iii) kirigami and origami designs, and (iv) nonplanar 3D fabrications. First, flexible substrates are the most common and intuitive methods, utilizing materials such as PDMS,[103,205,206] polyimides (PI),[207−210] FR4 (a class

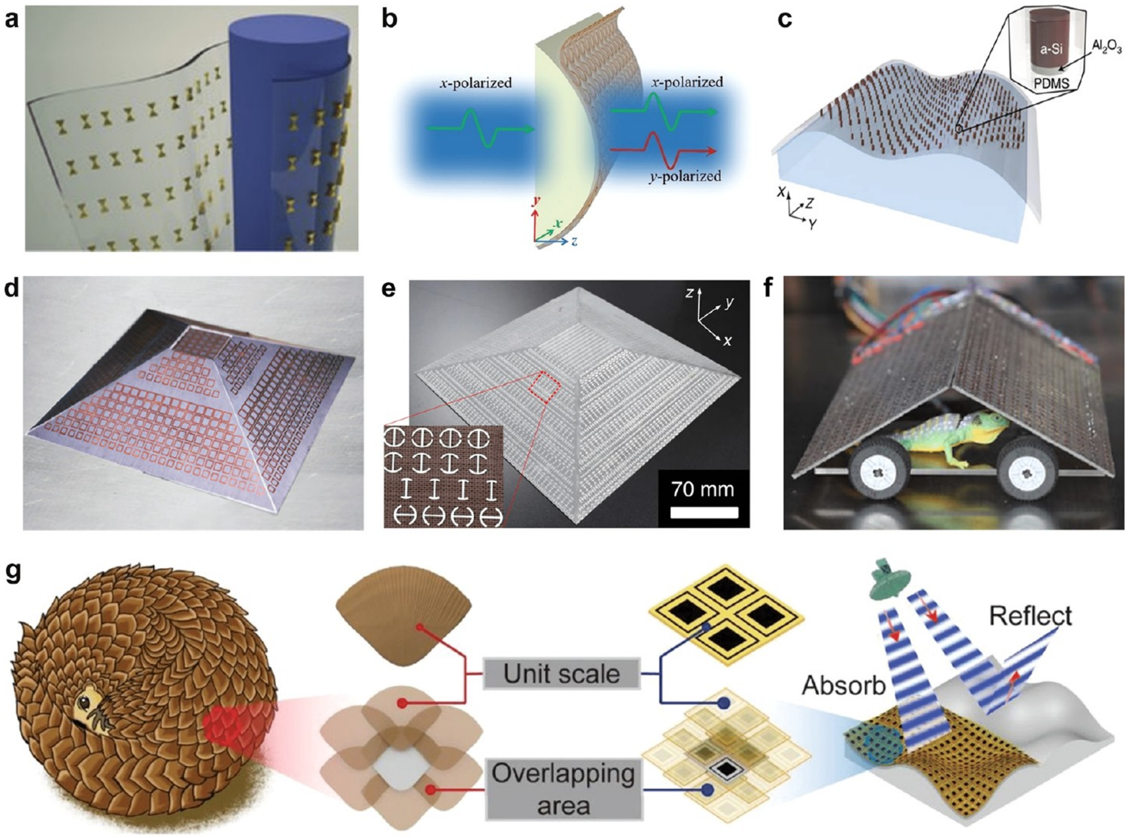

Figure 12. Conformal metasurfaces based on flexible substrates and multiplane approximations. (a) PDMS-enable conformal metasurface for an antenna. (b) PI-enable conformal metasurface for polarization division multiplexing. (c) PDMS-enable conformal metasurface for decoupling optical function and geometry of objects. (d) Top-cutting pyramid (5 planes) approximating arbitrary surface for full-polarization conformal metasurface cloak. (e) Top-cutting pyramid (5 planes) approximating arbitrary surface for polarization-insensitive conformal metasurface cloak. (f) Triangular bump composed by two planes for 3D metasurface cloak. (g) Pangolin-inspired soft-rigid-connection strategy for conformal metasurface cloak. (a) Reproduced with permission.[205] Copyright 2011, Wiley-VCH. (b) Reproduced with permission under a Creative Commons CC BY license from ref 105. Copyright 2018, Springer Nature. (c) Reproduced with permission.[210] Copyright 2020, Wiley-VCH. (d) Reproduced with permission.[113] Copyright 2016, Wiley-VCH. (e) Adapted with permission under a Creative Commons CC BY license from ref 214. Copyright 2021, Springer Nature. (f) Reproduced with permission.[106] Copyright 2020, Springer Nature. (g) Reproduced with permission.[215] Copyright 2021, Wiley-VCH.

of printed circuit board base material made from a flame retardant epoxy resin and glass fabric composite),[211] and poly(vinyl chloride) (PVC).[212] PDMS-based optical metasurfaces can actively adapt to curved surfaces by mechanically stretching the soft substrate (Figure 12a).[205] Meanwhile, due to the plasticity of PI/FR4/PVC, their corresponding metasurfaces can only bend and are limited to specific developable surfaces (Figure 12b).[210] Although serviceable, this strategy makes the design of optical elements complex and dependent on the surface geometry. To address such challenges, a theoretical framework for free-form conformal metasurfaces was proposed, exploiting transformation optics at the boundaries of arbitrary geometries.[213] Additionally, a modeling scheme was developed, utilizing conformal boundary optics and a modified finite-difference time-domain method, to design and simulate free-form metasurfaces with various geometries and functionalities (Figure 12c).[105]

Despite the generalization of theoretical and simulating methods for arbitrary surfaces, most of the proof-of-concept experiments and applications remain constrained to simple developable surfaces. As a makeshift solution, multiplane approximations have been introduced. The concept is akin to the infinite approximation of integral calculus. For example, Yang et al. used a pyramid without a top to mimic a hemispherical surface for a full-polarization 3D metasurface cloak (Figure 12d).[113] Similarly, Xu et al. also applied trapezoid and top-cutting pyramid platforms to approximate arbitrary shapes (Figure 12e).[214] As shown in Figures 12d and 12e, it consists of five planes. More simply, Qian et al. used a triangular bump composed of two planes for a 3D metasurface cloak (Figure 12f).[106] Although these concepts are adaptable to arbitrary surfaces, the experimental setups are planar, far from the desired free-form, interfacial, and full-polarization conformal metasurfaces for a realistic arbitrary object in practical applications. Recently, inspired by the scale-type skin of pangolin, Wang et al. presented a heuristic stretchable, conformable, and microwave-invisible metascale (Figure 12g).[215] The rigid electromagnetic dissipative unit cells were rationally deployed on a stretchable substrate. It should be noted that this design partly solves the conformal challenge. However, its ability to conform is fundamentally dependent on intrinsically soft materials.

Kirigami-based and origami-based conformal designs are recently emerging research directions, especially in flexible electronics.[98] In Figures 10c and 10d, kirigami and origami are utilized to form mechanically reconfigurable metasurfaces.

https://doi.org/10.1021/acsnano.3c09310
ACS Nano 2024, 18, 2685−2707

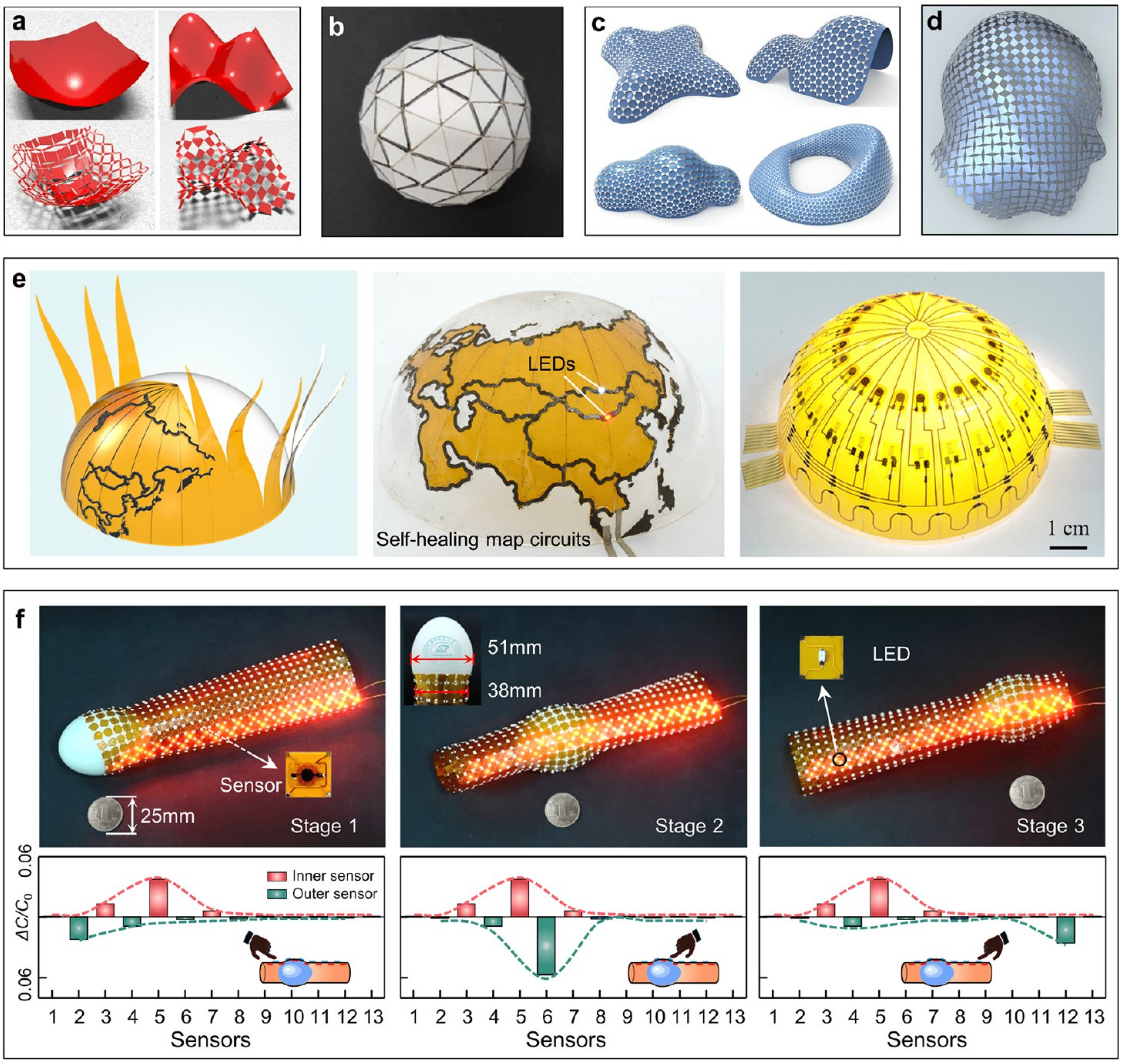

Figure 13. Kirigami-based and origami-based conformal metasurfaces. (a) Kirigami-based programming 3D surface fitting. (b) Origami-based computational wrapping of 3D-curved surfaces with nonstretchable materials. (c) Uniform-triangular-lattice kirigami-based computational conformability for different curved surfaces. (d) Inhomogeneous-square-lattice kirigami-based computational conformability. (e) Self-healing kirigami assembly strategy for conformal electronics. (f) Snakeskin-inspired, soft-hinge kirigami metamaterial for self-adaptive conformal electronic armor. (a) Reproduced with permission.[216] Copyright 2019, Springer Nature. (b) Adapted with permission under a Creative Commons CC BY license from ref 217. Copyright 2020, AAAS. (c) Reproduced with permission.[220] Copyright 2016, ACM. (d) Reproduced with permission.[221] Copyright 2021, Elsevier. (e) Reproduced with permission.[222] Copyright 2022, Wiley-VCH. (f) Reproduced with permission.[223] Copyright 2022, Wiley-VCH.

Additionally, they can also be underlying mechanisms for conformal metasurfaces. Their salient traits like negative Poisson's ratio and 2D-to-3D transformability offer interesting ideas for the conformal challenge. Kirigami and origami can eliminate the dependence on flexible substrates, rendering devices made of conventional rigid, nonstretchable, and even brittle materials (e.g., metals, silicons, and piezoelectrics) sufficiently conformable to wrap complex curved surfaces without failure. This is vital for conformal devices as current soft materials, such as PDMS and Ecoflex, are often limited by their low reliability and stability. Up to now, many paradigms have been presented. Choi et al. proposed an interesting generalized kirigami method under consideration of geometric and topological constraints, enabling the resultant kirigami tessellations to conform approximately to arbitrary prescribed curved surfaces (Figure 13a).[216] Lee et al. developed a computational origami strategy to realize the 3D conformal wrapping of complex curved surfaces with conventional rigid, nonstretchable materials (Figure 13b).[217] To overcome cut-induced discontinuities, Jin et al. further proposed a multilayer composite conformal approach.[218] Creatively, Konaković et al. merged computer graphics with 2D auxetic metasurface to achieve 3D conformal mappings, such as a uniform triangular lattice,[219] inhomogeneous triangular lattices (Figure 13c),[220] and inhomogeneous square lattice (Figure 13d).[221] Though more theoretical at present, this approach is likely to become a significant future direction.

In kirigami-based conformal designs, our team also has some thought-provoking attempts. The transformation of the 2D-to-3D mapping usually requires the material to be flexible and stretchable, which intrinsically conflicts with those devices made of nonstretchable materials that possess robust and high performances. We innovated by proposing a self-healing kirigami strategy, namely a hybrid material-structure strategy

https://doi.org/10.1021/acsnano.3c09310
ACS Nano 2024, 18, 2685−2707

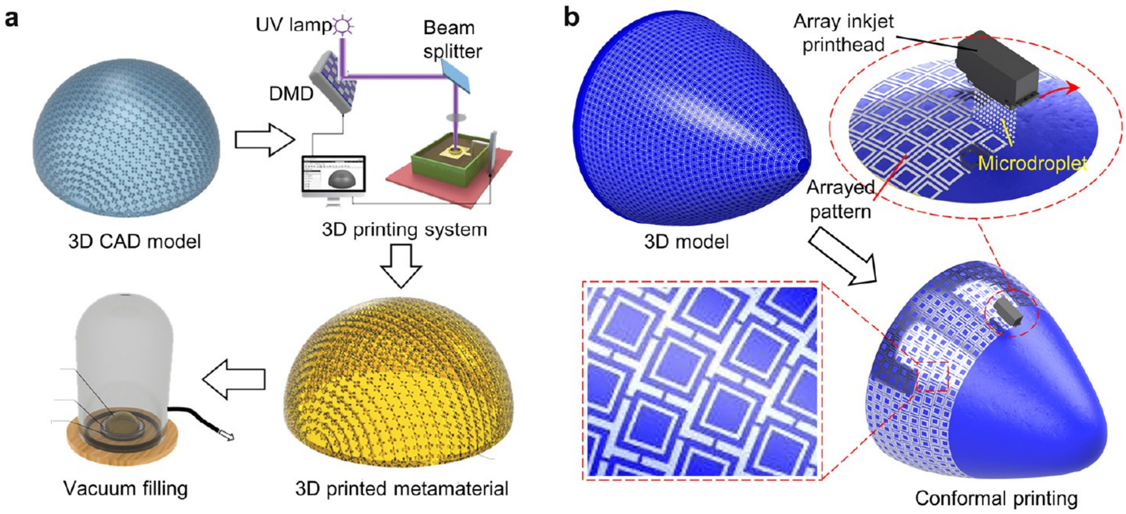

Figure 14. Nonplanar 3D fabrications for conformal metasurfaces. (a) 3D printed embedded metasurface by integrating PμSL 3D printing and the liquid metal filling method. (b) Conformal frequency-selective metasurface based on 5-axis 3D printing. (a) Reproduced with permission.[231] Copyright 2021, Wiley-VCH.

(Figure 13e, left).[222] Kirigami assembly was utilized to render the nonstretchable planar sheets sufficiently conformable to fully wrap a specific curved surface at the structural level, and the conductive self-healing materials were used to ensure the electrical conductivity of the functional materials to ensure device functionalities (Figure 13e, middle). In contrast to the previous approaches, this strategy is generically applicable to not only stretchable but also nonstretchable materials and assures the complete wrapping of conformal electronics with full areal coverage. We further conducted a combined theoretical and numerical analysis, along with experimental measurements, to gain insights into the mechanisms of conformal integration. Demonstrated applications in conformal heaters and multifunctional wind sensing systems on a sphere surface illustrate the promising application spectrum (Figure 13e, right). Besides, we described how snakeskin can serve as bioinspiration for employing electronic armor (E-armor) as a generic strategy to achieve flexibility, conformability, and protectability simultaneously.[223] Specifically, we developed a concept of flexible "E-armor" as an upgrade of soft "E-skin" in flexible electronics and soft robotics for this purpose. The soft-hinge kirigami mechanical metamaterial design ensures (i) protectability from rigid tiles, (ii) large areal coverage by auxetic stretchability, (iii) full conformability by overcoming the inherent bulking, and (iv) structural programmability without changing the rigid tiles. On this basis, tube-like electronic armor devices mimicking a snake swallowing prey provide simple examples of a wide spectrum of potential applications of this idea (Figure 13f).

Nonplanar 3D fabrications serve as the fourth approach to facilitate conformal metasurfaces or electronics, utilizing methods like 2D-to-3D transfer printing and conformal 3D printing. The 2D-to-3D transfer printing transfers devices based on planar technologies from a temporary flat substrate to a target curved surface, including elastomeric transfer printing,[224] water transfer printing,[225] multiscale transfer printing,[226] and conformal additive stamp printing.[227] However, these methods are still in their early stages, facing issues such as fragility, complexity, and low precision. As for conformal 3D printing, challenges are mainly concentrated on the materials selection and localization algorithm. In fact, inkjet printing is still strictly limited by unstable slurry-based materials that are unable to offer comparable performance available in conventional materials such as high conductivity and reliability.[227] On the other hand, there is significant research dedicated to developing conformal 3D printing algorithms. Alkadi et al. reported a conformal 3D slicing algorithm that generates data points based on the desired printing parameters (nozzle size, gap height, etc.).[228] Kucukdeger et al. propounded a nonplanar toolpath programming algorithm based on point cloud data representations of object topology.[229] Apart from that, Huang et al. put forward a programmable, mask-free robotized "transfer-and-jet" printing for large-area and complex-surface conformal fabrications.[230]

Two representative conformal metasurfaces are shown in Figure 14. One is 3D printed embedded metasurface, which integrates projection microstereolithography (PμSL) 3D printing and the liquid metal filling method (Figure 14a).[231] First, the 3D model with designated cavities is printed using PμSL, then liquid metals are injected into the cavities and subsequently sealed. This method, per se, realizes 3D conformal metasurface through conventional planar 3D printing, without considering the complex curved surfaces. It bypasses the challenges associated with nonplanar 3D fabrications and introduces a method for creating multilayer conformal metasurfaces that could significantly extend the operating band. Another representative conformal metasurface is fabricated by 5-axis inkjet printing, allowing for 5 degrees of freedom (Figure 14b). The system of structure−function integrated spray forming process includes a spray synchronous numerical control interpolation subsystem, a material spray control subsystem, a data processing and path planning subsystem, an infrared laser sintering subsystem, and a UV curing subsystem. The final conformal metasurface has a height of 400 mm and a max radius of 420 mm. Notably, the currently available fabrication techniques are mainly for passive optical metasurfaces. The techniques for actively tunable metasurfaces are virgin land.

6. OUTLOOK

Much like the success of their electronic analogs, research in flexible and conformal optical metasurfaces appears highly

https://doi.org/10.1021/acsnano.3c09310
ACS Nano 2024, 18, 2685−2707

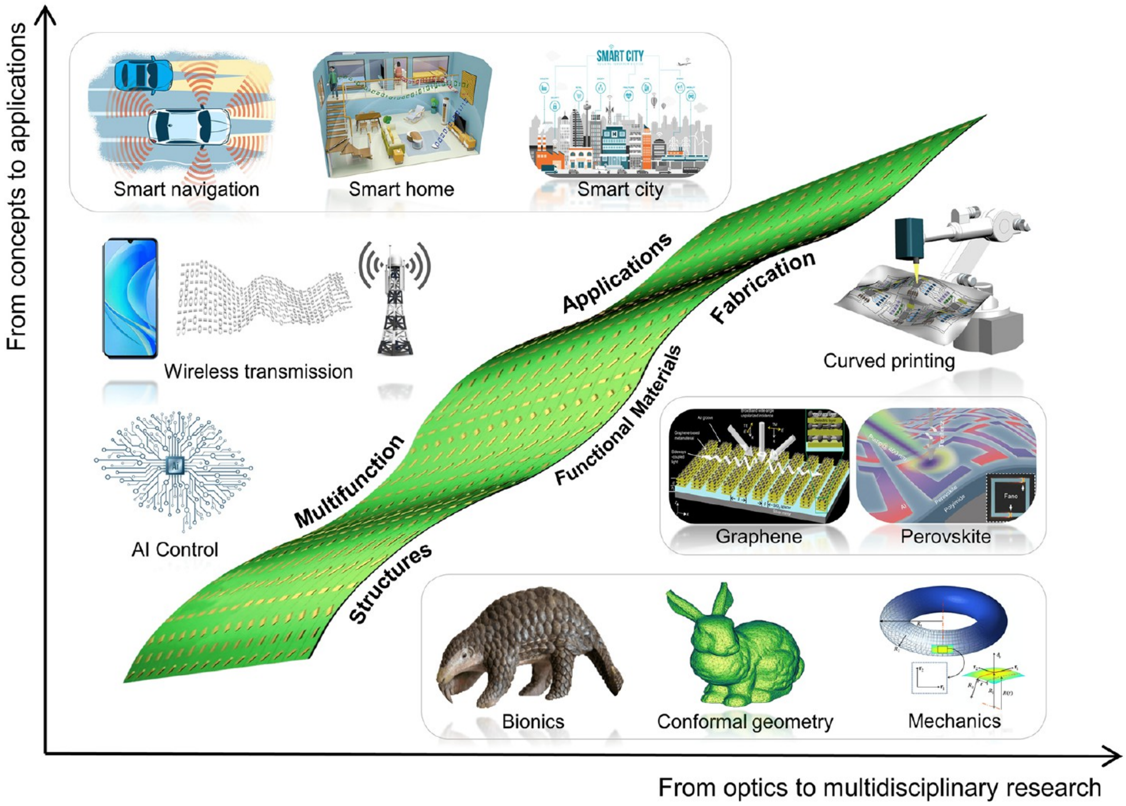

Figure 15. Future trends in flexible metasurfaces. Mechanics: a sheet mapping onto the surface of a torus. Reproduced with permission.[233] Copyright 2012, American Physical Society. Graphene: Graphene-based metasurface. Reproduced with permission.[234] Copyright 2019, Springer Nature. Perovskite: Perovskite-based metasurface. Reproduced with permission.[236] Copyright 2017, ACS. Curved printing: 3D curved electronics on complex surfaces. Adapted with permission under a Creative Commons CC BY license from ref 230. Copyright 2021, IOP. Smart home: Adapted with permission under a Creative Commons CC BY license from ref 237. Copyright 2020, Springer Nature.

promising. Fueled by the rapidly evolving advances in theoretical breakthroughs, computing methods, and micro/nanofabrication technologies, it has the potential to become a revolutionary technology to change the way of human life. As documented herein, the realization of flexible metasurfaces necessitates interdisciplinary research rather than only optics. The goal of this review, unlike many previous reviews of metasurfaces focusing on optical mechanisms, applications, or both, is to draw the attention of researchers from other disciplines and encourage their interests. To this end, we try to answer the questions: What are metasurfaces? Why are metasurfaces significant? why do we need metasurfaces to be flexible and conformal? How can we get flexible and conformal metasurfaces? This review serves as both a layman's guide to flexible metasurfaces and a specialist's insight into the wider possibilities of metasurfaces. On the other hand, this review shows more possibilities of metasurfaces to the specialists. Finally, we close this discussion by identifying several important branches for future work (Figure 15), mainly involving conformal structures (i.e., bionics,[223] conformal geometry,[232] and mechanics,[233] functional materials (i.e., graphene[234,235] and perovskite[236]), multifunction (i.e., AI control and wireless), curved fabrication,[230] and applications (i.e., smart navigation, smart home,[237] and smart city).

Although the quest has continued for a long time, the issue of conformality in film-based devices has not been adequately addressed. Many works claim their designs are conformal and can apply to arbitrary surfaces, but the authors have not seen any reports that can quantitatively describe the conformal behaviors, and even the metrics defining the conformability are still missing. Future research may focus on enhancing the reliability and stability of intrinsically stretchable materials, exploring kirigami-based and origami-based 2D-to-3D structural designs under the guidelines of mathematics and computer graphics, and achieving breakthroughs in conformal 3D fabrications. Additionally, areas like bionics and topological optimization warrant special attention. The bionic armors that have experienced evolution and refinement over millions of years provide great paradigms for conformal design. Historically, many great ideas in science and technology often arise from studying nature. Topological optimization has been proven an effective and powerful tool in structural engineering, but it has yet to reach its full potential. Particularly, the aspect of periodicity on curved surfaces is often overlooked and requires more focus, as periodicity defines metamaterials. Second, conformal coding metasurfaces have become an inevitable trend. The current coding metasurfaces are planar and rigid. Implementing optical property manipulation on complex and even arbitrary surfaces could benefit many applications. However, achieving this will necessitate overcoming challenges such as conformal circuit design and fabrication, multilayer interconnection and digital control, and the integration of numerous tiny chips. Third, conformal multifunctional metasurfaces are another main tributary. The complementarity of different functions and mutual verification of similar functions can greatly expand the scope of application and improve the system's robustness. Besides the aforementioned flexible electronics, flexible optical metasurfaces could

https://doi.org/10.1021/acsnano.3c09310
ACS Nano 2024, 18, 2685−2707

be integrated with other systems like energetics and thermotics, demanding bold conceptual innovation.

AUTHOR INFORMATION

Corresponding Authors

Shan Jiang − *Hangzhou Institute of Technology, Xidian University, Hangzhou 311200, China; School of Mechano-Electronic Engineering, Xidian University, Xi'an 710071, China*; Email: jiangshan@xidian.edu.cn

Jun Chen − *Department of Bioengineering, University of California, Los Angeles, Los Angeles, California 90095, United States*; orcid.org/0000-0002-3439-0495; Email: jun.chen@ucla.edu

Authors

Yunlei Zhou − *Hangzhou Institute of Technology, Xidian University, Hangzhou 311200, China; School of Mechano-Electronic Engineering, Xidian University, Xi'an 710071, China*; orcid.org/0000-0003-4645-4844

Shaolei Wang − *Department of Bioengineering, University of California, Los Angeles, Los Angeles, California 90095, United States*; orcid.org/0000-0001-8991-0550

Junyi Yin − *Department of Bioengineering, University of California, Los Angeles, Los Angeles, California 90095, United States*

Jianjun Wang − *Hangzhou Institute of Technology, Xidian University, Hangzhou 311200, China; School of Mechano-Electronic Engineering, Xidian University, Xi'an 710071, China*

Farid Manshaii − *Department of Bioengineering, University of California, Los Angeles, Los Angeles, California 90095, United States*

Xiao Xiao − *Department of Bioengineering, University of California, Los Angeles, Los Angeles, California 90095, United States*

Tianqi Zhang − *Hangzhou Institute of Technology, Xidian University, Hangzhou 311200, China; School of Mechano-Electronic Engineering, Xidian University, Xi'an 710071, China*

Hong Bao − *Hangzhou Institute of Technology, Xidian University, Hangzhou 311200, China; School of Mechano-Electronic Engineering, Xidian University, Xi'an 710071, China*

Complete contact information is available at:
https://pubs.acs.org/10.1021/acsnano.3c09310

Notes

The authors declare no competing financial interest.

ACKNOWLEDGMENTS

S. J. acknowledges the National Natural Science Foundation of China (Grant Nos. 52105575 & 52205593), the Fundamental Research Funds for the Central Universities (Grant No. QTZX23063), and the Proof of Concept Foundation of Xidian University Hangzhou Institute of Technology (Grant No. GNYZ2023YL0302). J.C. acknowledges the Henry Samueli School of Engineering & Applied Science and the Department of Bioengineering at the University of California, Los Angeles for the startup support. J.C. also acknowledges the Vernroy Makoto Watanabe Excellence in Research Award at the UCLA Samueli School of Engineering, the Brain & Behavior Research Foundation Young Investigator Grant (Grant Number: 30944).

VOCABULARY

Metasurface-based sensing: A resonance sensing mechanism that converts the target signals into electromagnetic resonance response.

Optical-metasurface-based healthcare: Healthcare by controlling electromagnetic fields in the vicinity of the human body.

Photonic skin: Flexible optical devices that mimic some characteristics of the skin by the light−matter interaction.

Multifunctional smart skin: Flexible devices that mimic some characteristics of the skin and incorporate the functions of flexible electronics, flexible optical metasurfaces, and so on.

Surface-enhanced Raman scattering: A surface-sensitive technique that enhances Raman scattering by molecules supported by metal surfaces or by nanostructures.

ABBREVIATIONS

ED, electric dipole; MD, magnetic dipole; EQ, electric quadrupole; MQ, magnetic quadrupole; SERS, surface-enhanced Raman scattering; OCT, optical coherence tomography; MRI, magnetic resonance imaging; SNR, signal-to-noise ratio; FPGA, field-programmable gate array; PDMS, polydimethylsiloxane; PI, polyimide; PVC, polyvinyl chloride; E-armor, electronic armor; PμSL, projection microstereolithography.

REFERENCES

(1) Kim, D.-H.; Lu, N.; Ma, R.; Kim, Y.-S.; Kim, R.-H.; Wang, S.; Wu, J.; Won, S. M.; Tao, H.; Islam, A.; Yu, K. J.; Kim, T.-i.; Chowdhury, R.; Ying, M.; Xu, L.; Li, M.; Chung, H.-J.; Keum, H.; McCormick, M.; Liu, P.; Zhang, Y.-W.; Omenetto, F. G.; Huang, Y.; Coleman, T.; Rogers, J. A. Epidermal Electronics. *Science* **2011**, *333* (6044), 838−843.

(2) Xu, J.; Tat, T.; Yin, J.; Ngo, D.; Zhao, X.; Wan, X.; Che, Z.; Chen, K.; Harris, L.; Chen, J. A textile magnetoelastic patch for self-powered personalized muscle physiotherapy. *Matter* **2023**, *6* (7), 2235−2247.

(3) Zhang, S.; Deng, Y.; Libanori, A.; Zhou, Y.; Yang, J.; Tat, T.; Yang, L.; Sun, W.; Zheng, P.; Zhu, Y. L.; Chen, J.; Tan, S. C. In Situ Grown Silver−Polymer Framework with Coordination Complexes for Functional Artificial Tissues. *Adv. Mater.* **2023**, *35*, 2207916.

(4) Meng, K.; Xiao, X.; Wei, W.; Chen, G.; Nashalian, A.; Shen, S.; Xiao, X.; Chen, J. Wearable pressure sensors for pulse wave monitoring. *Adv. Mater.* **2022**, *34* (21), 2109357.

(5) Zhao, X.; Chen, G.; Zhou, Y.; Nashalian, A.; Xu, J.; Tat, T.; Song, Y.; Libanori, A.; Xu, S.; Li, S.; Chen, J. Giant magnetoelastic effect enabled stretchable sensor for self-powered biomonitoring. *ACS Nano* **2022**, *16* (4), 6013−6022.

(6) Fang, Y.; Zhao, X.; Tat, T.; Xiao, X.; Chen, G.; Xu, J.; Chen, J. All-in-one conformal epidermal patch for multimodal biosensing. *Matter* **2021**, *4* (4), 1102−1105.

(7) Zhou, Z.; Chen, K.; Li, X.; Zhang, S.; Wu, Y.; Zhou, Y.; Meng, K.; Sun, C.; He, Q.; Fan, W.; Fan, E.; Lin, Z.; Tan, X.; Deng, W.; Yang, J.; Chen, J. Sign-to-speech translation using machine-learning-assisted stretchable sensor arrays. *Nat. Electron.* **2020**, *3* (9), 571−578.

(8) Yan, C.; Deng, W.; Jin, L.; Yang, T.; Wang, Z.; Chu, X.; Su, H.; Chen, J.; Yang, W. Epidermis-inspired ultrathin 3D cellular sensor array for self-powered biomedical monitoring. *ACS Appl. Mater. Interfaces* **2018**, *10* (48), 41070−41075.

(9) Zhao, T.; Xiao, X.; Wu, Y.; Ma, J.; Li, Y.; Lu, C.; Shokoohi, C.; Xu, Y.; Zhang, X.; Zhang, Y.; Ge, G.; Zhang, G.; Chen, J.; Zeng, Y. Tracing the Flu Symptom Progression via a Smart Face Mask. *Nano Lett.* **2023**, *23* (19), 8960−8969.

(10) Zhou, Y.; Zhao, X.; Xu, J.; Chen, G.; Tat, T.; Li, J.; Chen, J. A multimodal magnetoelastic artificial skin for underwater haptic sensing. *Sci. Adv.* **2024**, *10* (1), eadj8567.

(11) Su, Y.; Liu, Y.; Li, W.; Xiao, X.; Chen, C.; Lu, H.; Yuan, Z.; Tai, H.; Jiang, Y.; Zou, J.; Xie, G.; Chen, J. Sensing−transducing coupled piezoelectric textiles for self-powered humidity detection and wearable biomonitoring. *Mater. Horiz.* **2023**, *10* (3), 842−851.

(12) Pan, H.; Chen, G.; Chen, Y.; Di Carlo, A.; Mayer, M. A.; Shen, S.; Chen, C.; Li, W.; Subramaniam, S.; Huang, H.; Tai, H.; Jiang, Y.; Xie, G.; Su, Y.; Chen, J. Biodegradable cotton fiber-based piezoresistive textiles for wearable biomonitoring. *Biosens. Bioelectron.* **2023**, *222*, 114999.

(13) Tat, T.; Chen, G.; Zhao, X.; Zhou, Y.; Xu, J.; Chen, J. Smart textiles for healthcare and sustainability. *ACS Nano* **2022**, *16* (9), 13301−13313.

(14) Libanori, A.; Chen, G.; Zhao, X.; Zhou, Y.; Chen, J. Smart textiles for personalized healthcare. *Nat. Electron.* **2022**, *5* (3), 142−156.

(15) Zhao, X.; Zhou, Y.; Xu, J.; Chen, G.; Fang, Y.; Tat, T.; Xiao, X.; Song, Y.; Li, S.; Chen, J. Soft fibers with magnetoelasticity for wearable electronics. *Nat. Commun.* **2021**, *12* (1), 6755.

(16) Chen, G.; Zhao, X.; Andalib, S.; Xu, J.; Zhou, Y.; Tat, T.; Lin, K.; Chen, J. Discovering giant magnetoelasticity in soft matter for electronic textiles. *Matter* **2021**, *4* (11), 3725−3740.

(17) Xiao, X.; Xiao, X.; Nashalian, A.; Libanori, A.; Fang, Y.; Li, X.; Chen, J. Triboelectric nanogenerators for self-powered wound healing. *Adv. Healthcare Mater.* **2021**, *10* (20), 2100975.

(18) Su, Y.; Chen, C.; Pan, H.; Yang, Y.; Chen, G.; Zhao, X.; Li, W.; Gong, Q.; Xie, G.; Zhou, Y.; Zhang, S.; Tai, H.; Jiang, Y.; Chen, J. Muscle fibers inspired high-performance piezoelectric textiles for wearable physiological monitoring. *Adv. Funct. Mater.* **2021**, *31* (19), 2010962.

(19) Fang, Y.; Zhao, X.; Chen, G.; Tat, T.; Chen, J. Smart polyethylene textiles for radiative and evaporative cooling. *Joule* **2021**, *5* (4), 752−754.

(20) Su, Y.; Liu, Z.; Xu, L. An Universal and Easy-to-Use Model for the Pressure of Arbitrary-Shape 3D Multifunctional Integumentary Cardiac Membranes. *Adv. Healthcare Mater.* **2016**, *5* (8), 889−892.

(21) Abiri, P.; Duarte-Vogel, S.; Chou, T.-C.; Abiri, A.; Gudapati, V.; Yousefi, A.; Roustaei, M.; Chang, C.-C.; Cui, Q.; Hsu, J. J.; Bersohn, M.; Markovic, D.; Chen, J.; Tai, Y.-C.; Hsiai, T. K. *In vivo* intravascular pacing using a wireless microscale stimulator. *Ann. Biomed. Eng.* **2021**, *49*, 2094.

(22) Wang, S.; Nie, Y.; Zhu, H.; Xu, Y.; Cao, S.; Zhang, J.; Li, Y.; Wang, J.; Ning, X.; Kong, D. Intrinsically stretchable electronics with ultrahigh deformability to monitor dynamically moving organs. *Sci. Adv.* **2022**, *8* (13), eabl5511.

(23) Wang, S.; Cui, Q.; Abiri, P.; Roustaei, M.; Zhu, E.; Li, Y.-R.; Wang, K.; Duarte, S.; Yang, L.; Ebrahimi, R.; Bersohn, M.; Chen, J.; Hsiai, T. A self-assembled implantable microtubular pacemaker for wireless cardiac electrotherapy. *Sci. Adv.* **2023**, *9* (42), eadj0540.

(24) Che, Z.; O'Donovan, S.; Xiao, X.; Wan, X.; Chen, G.; Zhao, X.; Zhou, Y.; Yin, J.; Chen, J. Implantable Triboelectric Nanogenerators for Self-Powered Cardiovascular Healthcare. *Small* **2023**, *19*, 2207600.

(25) Zhou, Y.; Zhao, X.; Xu, J.; Fang, Y.; Chen, G.; Song, Y.; Li, S.; Chen, J. Giant magnetoelastic effect in soft systems for bioelectronics. *Nat. Mater.* **2021**, *20* (12), 1670−1676.

(26) Fang, Y.; Zou, Y.; Xu, J.; Chen, G.; Zhou, Y.; Deng, W.; Zhao, X.; Roustaei, M.; Hsiai, T. K.; Chen, J. Ambulatory cardiovascular monitoring via a machine-learning-assisted textile triboelectric sensor. *Adv. Mater.* **2021**, *33* (41), 2104178.

(27) Guo, R.; Fang, Y.; Wang, Z.; Libanori, A.; Xiao, X.; Wan, D.; Cui, X.; Sang, S.; Zhang, W.; Zhang, H.; Chen, J. Deep learning assisted body area triboelectric hydrogel sensor network for infant care. *Adv. Funct. Mater.* **2022**, *32* (35), 2204803.

(28) Zhou, Y.; Xiao, X.; Chen, G.; Zhao, X.; Chen, J. Self-powered sensing technologies for human Metaverse interfacing. *Joule* **2022**, *6* (7), 1381−1389.

(29) Alagumalai, A.; Shou, W.; Mahian, O.; Aghbashlo, M.; Tabatabaei, M.; Wongwises, S.; Liu, Y.; Zhan, J.; Torralba, A.; Chen, J.; Wang, Z.; Matusik, W. Self-powered sensing systems with learning capability. *Joule* **2022**, *6*, 1475.

(30) Fang, Y.; Xu, J.; Xiao, X.; Zou, Y.; Zhao, X.; Zhou, Y.; Chen, J. A Deep-Learning-Assisted On-Mask Sensor Network for Adaptive Respiratory Monitoring. *Adv. Mater.* **2022**, *34* (24), 2200252.

(31) Xiao, X.; Yin, J.; Chen, G.; Shen, S.; Nashalian, A.; Chen, J. Bioinspired acoustic textiles with nanoscale vibrations for wearable biomonitoring. *Matter* **2022**, *5* (5), 1342−1345.

(32) Zhai, Y.; Li, J.; Shen, S.; Zhu, Z.; Mao, S.; Xiao, X.; Zhu, C.; Tang, J.; Lu, X.; Chen, J. Recent Advances on Dual-Band Electrochromic Materials and Devices. *Adv. Funct. Mater.* **2022**, *32* (17), 2109848.

(33) Xu, J.; Yin, J.; Fang, Y.; Xiao, X.; Zou, Y.; Wang, S.; Chen, J. Deep learning assisted ternary electrification layered triboelectric membrane sensor for self-powered home security. *Nano Energy* **2023**, *113*, 108524.

(34) Xiao, X.; Fang, Y.; Xiao, X.; Xu, J.; Chen, J. Machine-learning-aided self-powered assistive physical therapy devices. *ACS Nano* **2021**, *15* (12), 18633−18646.

(35) Conta, G.; Libanori, A.; Tat, T.; Chen, G.; Chen, J. Triboelectric nanogenerators for therapeutic electrical stimulation. *Adv. Mater.* **2021**, *33* (26), 2007502.

(36) Fang, Y.; Chen, G.; Bick, M.; Chen, J. Smart textiles for personalized thermoregulation. *Chem. Soc. Rev.* **2021**, *50* (17), 9357−9374.

(37) Jiang, S.; Zhang, T.; Zhou, Y.; Lai, P.; Huang, Y. Wearable ultrasound bioelectronics for healthcare monitoring. *Innovation* **2023**, *4* (4), 100447.

(38) Zhang, T.; Liu, N.; Xu, J.; Liu, Z.; Zhou, Y.; Yang, Y.; Li, S.; Huang, Y.; Jiang, S. Flexible electronics for cardiovascular healthcare monitoring. *Innovation* **2023**, *4* (5), 100485.

(39) Li, Y.; Yin, J.; Liu, S.; Xue, B.; Shokoohi, C.; Ge, G.; Hu, M.; Li, T.; Tao, X.; Rao, Z.; et al. Learning Hand Kinematics for Parkinson's Disease Assessment Using a Multimodal Sensor Glove. *Adv. Sci.* **2023**, *10*, 2206982.

(40) Meng, F.; Liu, C.; Li, Y.; Hao, H.; Li, Q.; Lyu, C.; Wang, Z.; Ge, G.; Yin, J.; Ji, X.; Xiao, X. Personalized and Safe Soft Glove for Rehabilitation Training. *Electronics* **2023**, *12* (11), 2531.

(41) Shen, S.; Xiao, X.; Yin, J.; Xiao, X.; Chen, J. Self-Powered Smart Gloves Based on Triboelectric Nanogenerators. *Small Methods* **2022**, *6* (10), 2200830.

(42) Meng, K.; Xiao, X.; Liu, Z.; Shen, S.; Tat, T.; Wang, Z.; Lu, C.; Ding, W.; He, X.; Yang, J.; Chen, J. Kirigami-Inspired Pressure Sensors for Wearable Dynamic Cardiovascular Monitoring. *Adv. Mater.* **2022**, *34* (36), 2202478.

(43) Deng, W.; Zhou, Y.; Libanori, A.; Chen, G.; Yang, W.; Chen, J. Piezoelectric nanogenerators for personalized healthcare. *Chem. Soc. Rev.* **2022**, *51*, 3380.

(44) Chen, G.; Xiao, X.; Zhao, X.; Tat, T.; Bick, M.; Chen, J. Electronic textiles for wearable point-of-care systems. *Chem. Rev.* **2022**, *122* (3), 3259−3291.

(45) Su, Y.; Chen, G.; Chen, C.; Gong, Q.; Xie, G.; Yao, M.; Tai, H.; Jiang, Y.; Chen, J. Self-powered respiration monitoring enabled by a triboelectric nanogenerator. *Adv. Mater.* **2021**, *33* (35), 2101262.

(46) Chen, G.; Shen, S.; Tat, T.; Zhao, X.; Zhou, Y.; Fang, Y.; Chen, J. Wearable respiratory sensors for COVID-19 monitoring. *View* **2022**, *3* (5), 20220024.

(47) Li, J.; Xia, B.; Xiao, X.; Huang, Z.; Yin, J.; Jiang, Y.; Wang, S.; Gao, H.; Shi, Q.; Xie, Y.; Chen, J. Stretchable Thermoelectric Fibers with Three-Dimensional Interconnected Porous Network for Low-Grade Body Heat Energy Harvesting. *ACS Nano* **2023**, *17* (19), 19232−19241.

(48) Xu, J.; Tat, T.; Zhao, X.; Xiao, X.; Zhou, Y.; Yin, J.; Chen, K.; Chen, J. Spherical Magnetoelastic Generator for Multidirectional Vibration Energy Harvesting. *ACS Nano* **2023**, *17* (4), 3865−3872.

(49) Zhao, X.; Chang, A.; Li, J.; Xu, J.; Hollister, J.; Che, Z.; Wan, X.; Yin, J.; Wang, S.; Lee, S.; Kavehpour, P.; Chen, J. Air-Permeable

Textile Bioelectronics for Wearable Energy Harvesting and Active Sensing. *Adv. Mater. Technol.* **2023**, *8* (8), 2201703.
(50) Ock, I. W.; Zhao, X.; Wan, X.; Zhou, Y.; Chen, G.; Chen, J. Boost the voltage of a magnetoelastic generator via tuning the magnetic induction layer resistance. *Nano Energy* **2023**, *109*, 108298.
(51) Sun, Y.; Shen, S.; Deng, W.; Tian, G.; Xiong, D.; Zhang, H.; Yang, T.; Wang, S.; Chen, J.; Yang, W. Suppressing piezoelectric screening effect at atomic scale for enhanced piezoelectricity. *Nano Energy* **2023**, *105*, 108024.
(52) Xu, J.; Tat, T.; Zhao, X.; Zhou, Y.; Ngo, D.; Xiao, X.; Chen, J. A Programable Magnetoelastic Sensor Array for Self-Powered Human-Machine Interface. *Appl. Phys. Rev.* **2022**, *9*, No. 031404.
(53) Alagumalai, A.; Mahian, O.; Vimal, K.; Yang, L.; Xiao, X.; Saeidi, S.; Zhang, P.; Saboori, T.; Wongwises, S.; Wang, Z. L.; Chen, J. A contextual framework development toward triboelectric nanogenerator commercialization. *Nano Energy* **2022**, *101*, 107572.
(54) Chang, A.; Uy, C.; Xiao, X.; Xiao, X.; Chen, J. Self-powered environmental monitoring via a triboelectric nanogenerator. *Nano Energy* **2022**, *98*, 107282.
(55) Lan, B.; Xiao, X.; Carlo, A. D.; Deng, W.; Yang, T.; Jin, L.; Tian, G.; Ao, Y.; Yang, W.; Chen, J. Topological nanofibers enhanced piezoelectric membranes for soft bioelectronics. *Adv. Funct. Mater.* **2022**, *32* (49), 2207393.
(56) Chen, G.; Li, Y.; Bick, M.; Chen, J. Smart textiles for electricity generation. *Chem. Rev.* **2020**, *120* (8), 3668−3720.
(57) Yang, G.-Z.; Bellingham, J.; Dupont, P. E.; Fischer, P.; Floridi, L.; Full, R.; Jacobstein, N.; Kumar, V.; McNutt, M.; Merrifield, R.; et al. The grand challenges of Science Robotics. *Sci. Robot.* **2018**, *3* (14), eaar7650.
(58) Li, Y.; Wang, S.; Zhang, J.; Ma, X.; Cao, S.; Sun, Y.; Feng, S.; Fang, T.; Kong, D. A Highly Stretchable and Permeable Liquid Metal Micromesh Conductor by Physical Deposition for Epidermal Electronics. *ACS Appl. Mater. Interfaces* **2022**, *14* (11), 13713−13721.
(59) Hu, G.; Wang, S.; Yu, J.; Zhang, J.; Sun, Y.; Kong, D. A facile and scalable patterning approach for ultrastretchable liquid metal features. *Lab Chip* **2022**, *22* (24), 4933−4940.
(60) Ma, H.; Qin, H.; Xiao, X.; Liu, N.; Wang, S.; Li, J.; Shen, S.; Dai, S.; Sun, M.; Li, P.; et al. Robust hydrogel sensors for unsupervised learning enabled sign-to-verbal translation. *InfoMat* **2023**, *5*, e12419.
(61) Xu, J.; Tat, T.; Zhao, X.; Zhou, Y.; Ngo, D.; Xiao, X.; Chen, J. A programmable magnetoelastic sensor array for self-powered human−machine interface. *Appl. Phys. Rev.* **2022**, DOI: 10.1063/5.0094289.
(62) Xiong, W.; Feng, H.; Liwang, H.; Li, D.; Yao, W.; Duolikun, D.; Zhou, Y.; Huang, Y. Multifunctional Tactile Feedbacks Towards Compliant Robot Manipulations via 3D-Shaped Electronic Skin. *IEEE Sens. J.* **2022**, *22* (9), 9046−9056.
(63) Huang, Y.; Zhu, C.; Xiong, W.; Wang, Y.; Jiang, Y.; Qiu, L.; Guo, D.; Hou, C.; Jiang, S.; Yang, Z.; et al. Flexible smart sensing skin for "Fly-by-Feel" morphing aircraft. *Sci. China: Technol. Sci.* **2022**, *65*, 1−29.
(64) Xiong, W.; Zhu, C.; Guo, D.; Hou, C.; Yang, Z.; Xu, Z.; Qiu, L.; Yang, H.; Li, K.; Huang, Y. Bio-inspired, intelligent flexible sensing skin for multifunctional flying perception. *Nano Energy* **2021**, *90*, 106550.
(65) Xiong, W.; Guo, D.; Yang, Z.; Zhu, C.; Huang, Y. Conformable, programmable and step-linear sensor array for large-range wind pressure measurement on curved surface. *Sci. China: Technol. Sci.* **2020**, *63* (10), 2073−2081.
(66) Geiger, S.; Michon, J.; Liu, S.; Qin, J.; Ni, J.; Hu, J.; Gu, T.; Lu, N. Flexible and stretchable photonics: the next stretch of opportunities. *ACS Photonics* **2020**, *7* (10), 2618−2635.
(67) Jin, P.; Fu, J.; Wang, F.; Zhang, Y.; Wang, P.; Liu, X.; Jiao, Y.; Li, H.; Chen, Y.; Ma, Y.; Feng, X. A flexible, stretchable system for simultaneous acoustic energy transfer and communication. *Sci. Adv.* **2021**, *7* (40), eabg2507.
(68) Lin, Z.; Zhang, G.; Xiao, X.; Au, C.; Zhou, Y.; Sun, C.; Zhou, Z.; Yan, R.; Fan, E.; Si, S.; et al. A personalized acoustic interface for wearable human−machine interaction. *Adv. Funct. Mater.* **2022**, *32* (9), 2109430.
(69) Bertoldi, K.; Vitelli, V.; Christensen, J.; Van Hecke, M. Flexible mechanical metamaterials. *Nat. Rev. Mater.* **2017**, *2* (11), 17066.
(70) Mayer, M.; Xiao, X.; Yin, J.; Chen, G.; Xu, J.; Chen, J. Advances in Bioinspired Triboelectric Nanogenerators. *Adv. Electron. Mater.* **2022**, *8*, 2200782.
(71) Gao, Z.; Xiao, X.; Carlo, A. D.; Yin, J.; Wang, Y.; Huang, L.; Tang, J.; Chen, J. Advances in wearable strain sensors based on electrospun fibers. *Adv. Funct. Mater.* **2023**, *33* (18), 2214265.
(72) Yin, J.; Wang, S.; Di Carlo, A.; Chang, A.; Wan, X.; Xu, J.; Xiao, X.; Chen, J. Smart textiles for self-powered biomonitoring. *Med-X* **2023**, *1*, 3.
(73) Zhang, Z.; Xiao, X.; Zhou, Y.; Huang, L.; Wang, Y.; Rong, Q.; Han, Z.; Qu, H.; Zhu, Z.; Xu, S.; Tang, J.; Chen, J. Bioinspired graphene oxide membranes with pH-responsive nanochannels for high-performance nanofiltration. *ACS Nano* **2021**, *15* (8), 13178−13187.
(74) Su, Y.; Wang, J.; Wang, B.; Yang, T.; Yang, B.; Xie, G.; Zhou, Y.; Zhang, S.; Tai, H.; Cai, Z.; et al. Alveolus-inspired active membrane sensors for self-powered wearable chemical sensing and breath analysis. *ACS Nano* **2020**, *14* (5), 6067−6075.
(75) Bai, P.; Zhu, G.; Jing, Q.; Yang, J.; Chen, J.; Su, Y.; Ma, J.; Zhang, G.; Wang, Z. L. Membrane-based self-powered triboelectric sensors for pressure change detection and its uses in security surveillance and healthcare monitoring. *Adv. Funct. Mater.* **2014**, *24* (37), 5807−5813.
(76) Zhu, G.; Su, Y.; Bai, P.; Chen, J.; Jing, Q.; Yang, W.; Wang, Z. L. Harvesting water wave energy by asymmetric screening of electrostatic charges on a nanostructured hydrophobic thin-film surface. *ACS Nano* **2014**, *8* (6), 6031−6037.
(77) Xiao, X.; Xiao, X.; Zhou, Y.; Zhao, X.; Chen, G.; Liu, Z.; Wang, Z.; Lu, C.; Hu, M.; Nashalian, A.; Shen, S.; Xie, K.; Yang, W.; Gong, Y.; Ding, W.; Servati, P.; Han, C.; Dou, S. X.; Li, W.; Chen, J. An ultrathin rechargeable solid-state zinc ion fiber battery for electronic textiles. *Sci. Adv.* **2021**, *7* (49), eabl3742.
(78) Wan, J.; Xie, J.; Kong, X.; Liu, Z.; Liu, K.; Shi, F.; Pei, A.; Chen, H.; Chen, W.; Chen, J.; Zhang, X.; Zong, L.; Wang, J.; Chen, L.-Q.; Qin, J.; Cui, Y. Ultrathin, flexible, solid polymer composite electrolyte enabled with aligned nanoporous host for lithium batteries. *Nat. Nanotechnol.* **2019**, *14* (7), 705−711.
(79) Fan, X.; Chen, J.; Yang, J.; Bai, P.; Li, Z.; Wang, Z. L. Ultrathin, rollable, paper-based triboelectric nanogenerator for acoustic energy harvesting and self-powered sound recording. *ACS Nano* **2015**, *9* (4), 4236−4243.
(80) Chang, S.; Guo, X.; Ni, X. Optical metasurfaces: progress and applications. *Annu. Rev. Mater. Res.* **2018**, *48* (1), 279−302.
(81) Lee, H.; Lee, J. K.; Seung, H. M.; Kim, Y. Y. Mass-stiffness substructuring of an elastic metasurface for full transmission beam steering. *J. Mech. Phys. Solids* **2018**, *112*, 577−593.
(82) Assouar, B.; Liang, B.; Wu, Y.; Li, Y.; Cheng, J.-C.; Jing, Y. Acoustic metasurfaces. *Nat. Rev. Mater.* **2018**, *3* (12), 460−472.
(83) Guo, J.; Xu, G.; Tian, D.; Qu, Z.; Qiu, C. W. A Real-Time Self-Adaptive Thermal Metasurface. *Adv. Mater.* **2022**, *34* (24), 2201093.
(84) Hsiao, H. H.; Chu, C. H.; Tsai, D. P. Fundamentals and applications of metasurfaces. *Small Methods* **2017**, *1* (4), 1600064.
(85) Shi, Q.; Dong, B.; He, T.; Sun, Z.; Zhu, J.; Zhang, Z.; Lee, C. Progress in wearable electronics/photonics—Moving toward the era of artificial intelligence and internet of things. *InfoMat* **2020**, *2* (6), 1131−1162.
(86) Wang, Y.; Zhao, C.; Wang, J.; Luo, X.; Xie, L.; Zhan, S.; Kim, J.; Wang, X.; Liu, X.; Ying, Y. Wearable plasmonic-metasurface sensor for noninvasive and universal molecular fingerprint detection on biointerfaces. *Sci. Adv.* **2021**, *7* (4), eabe4553.
(87) Li, Z.; Tian, X.; Qiu, C.-W.; Ho, J. S. Metasurfaces for bioelectronics and healthcare. *Nat. Electron.* **2021**, *4*, 382.
(88) Tian, X.; Lee, P. M.; Tan, Y. J.; Wu, T. L.; Yao, H.; Zhang, M.; Li, Z.; Ng, K. A.; Tee, B. C.; Ho, J. S. Wireless body sensor networks based on metamaterial textiles. *Nat. Electron.* **2019**, *2* (6), 243−251.

(89) Hajiaghajani, A.; Afandizadeh Zargari, A. H.; Dautta, M.; Jimenez, A.; Kurdahi, F.; Tseng, P. Textile-integrated metamaterials for near-field multibody area networks. *Nat. Electron.* **2021**, *4*, 808−817.

(90) Su, V.-C.; Chu, C. H.; Sun, G.; Tsai, D. P. Advances in optical metasurfaces: fabrication and applications. *Opt. Express* **2018**, *26* (10), 13148−13182.

(91) Hu, J.; Bandyopadhyay, S.; Liu, Y.-h.; Shao, L.-y. A review on metasurface: from principle to smart metadevices. *Front. Phys.* **2021**, *8*, 586087.

(92) Li, G.; Zhang, S.; Zentgraf, T. Nonlinear photonic metasurfaces. *Nat. Rev. Mater.* **2017**, *2* (5), 1−14.

(93) Li, L.; Zhao, H.; Liu, C.; Li, L.; Cui, T. J. Intelligent metasurfaces: control, communication and computing. *eLight* **2022**, *2* (1), 1−24.

(94) Qiu, C.-W.; Zhang, T.; Hu, G.; Kivshar, Y. Quo vadis, metasurfaces? *Nano Lett.* **2021**, *21* (13), 5461−5474.

(95) Zhang, S.; Zhou, Y.; Libanori, A.; Deng, Y.; Liu, M.; Zhou, M.; Qu, H.; Zhao, X.; Zheng, P.; Zhu, Y.-L.; et al. Biomimetic spinning of soft functional fibres via spontaneous phase separation. *Nat. Electron.* **2023**, *6*, 338−348.

(96) Luo, Y.; Abidian, M. R.; Ahn, J.-H.; Akinwande, D.; Andrews, A. M.; Antonietti, M.; Bao, Z.; Berggren, M.; Berkey, C. A.; Bettinger, C. J.; et al. Technology roadmap for flexible sensors. *ACS Nano* **2023**, *17* (6), 5211−5295.

(97) Xu, J.; Cai, H.; Wu, Z.; Li, X.; Tian, C.; Ao, Z.; Niu, V. C.; Xiao, X.; Jiang, L.; Khodoun, M.; et al. Acoustic metamaterials-driven transdermal drug delivery for rapid and on-demand management of acute disease. *Nat. Commun.* **2023**, *14* (1), 869.

(98) Jiang, S.; Liu, X.; Liu, J.; Ye, D.; Duan, Y.; Li, K.; Yin, Z.; Huang, Y. Flexible Metamaterial Electronics. *Adv. Mater.* **2022**, *34*, 2200070.

(99) Yu, N.; Genevet, P.; Kats, M. A.; Aieta, F.; Tetienne, J.-P.; Capasso, F.; Gaburro, Z. Light propagation with phase discontinuities: generalized laws of reflection and refraction. *Science* **2011**, *334* (6054), 333−337.

(100) Ni, X.; Emani, N. K.; Kildishev, A. V.; Boltasseva, A.; Shalaev, V. M. Broadband light bending with plasmonic nanoantennas. *Science* **2012**, *335* (6067), 427−427.

(101) Cui, T. J.; Qi, M. Q.; Wan, X.; Zhao, J.; Cheng, Q. Coding metamaterials, digital metamaterials and programmable metamaterials. *Light: Sci. Appl.* **2014**, *3* (10), e218−e218.

(102) Ni, X.; Wong, Z. J.; Mrejen, M.; Wang, Y.; Zhang, X. An ultrathin invisibility skin cloak for visible light. *Science* **2015**, *349* (6254), 1310−1314.

(103) Kamali, S. M.; Arbabi, A.; Arbabi, E.; Horie, Y.; Faraon, A. Decoupling optical function and geometrical form using conformal flexible dielectric metasurfaces. *Nat. Commun.* **2016**, *7* (1), 11618.

(104) Wang, Z.; Jing, L.; Yao, K.; Yang, Y.; Zheng, B.; Soukoulis, C. M.; Chen, H.; Liu, Y. Origami-based reconfigurable metamaterials for tunable chirality. *Adv. Mater.* **2017**, *29* (27), 1700412.

(105) Wu, K.; Coquet, P.; Wang, Q. J.; Genevet, P. Modelling of free-form conformal metasurfaces. *Nat. Commun.* **2018**, *9* (1), 1−8.

(106) Qian, C.; Zheng, B.; Shen, Y.; Jing, L.; Li, E.; Shen, L.; Chen, H. Deep-learning-enabled self-adaptive microwave cloak without human intervention. *Nat. Photonics* **2020**, *14* (6), 383−390.

(107) Liu, C.; Ma, Q.; Luo, Z. J.; Hong, Q. R.; Xiao, Q.; Zhang, H. C.; Miao, L.; Yu, W. M.; Cheng, Q.; Li, L.; Cui, T. J. A programmable diffractive deep neural network based on a digital-coding metasurface array. *Nat. Electron.* **2022**, *5* (2), 113−122.

(108) Liu, X.; Wang, J.; Tang, L.; Xie, L.; Ying, Y. Flexible Plasmonic Metasurfaces with User-Designed Patterns for Molecular Sensing and Cryptography. *Adv. Funct. Mater.* **2016**, *26* (30), 5515−5523.

(109) Evlyukhin, A. B.; Novikov, S. M.; Zywietz, U.; Eriksen, R. L.; Reinhardt, C.; Bozhevolnyi, S. I.; Chichkov, B. N. Demonstration of magnetic dipole resonances of dielectric nanospheres in the visible region. *Nano Lett.* **2012**, *12* (7), 3749−3755.

(110) Kruk, S.; Kivshar, Y. Functional meta-optics and nanophotonics governed by Mie resonances. *ACS Photonics* **2017**, *4* (11), 2638−2649.

(111) Kivshar, Y.; Miroshnichenko, A. Meta-optics with Mie resonances. *Opt. Photonics News* **2017**, *28* (1), 24−31.

(112) Liu, T.; Xu, R.; Yu, P.; Wang, Z.; Takahara, J. Multipole and multimode engineering in Mie resonance-based metastructures. *Nanophotonics* **2020**, *9* (5), 1115−1137.

(113) Yang, Y.; Jing, L.; Zheng, B.; Hao, R.; Yin, W.; Li, E.; Soukoulis, C. M.; Chen, H. Full-polarization 3D metasurface cloak with preserved amplitude and phase. *Adv. Mater.* **2016**, *28* (32), 6866−6871.

(114) Ma, Q.; Bai, G. D.; Jing, H. B.; Yang, C.; Li, L.; Cui, T. J. Smart metasurface with self-adaptively reprogrammable functions. *Light: Sci. Appl.* **2019**, *8* (1), 1−12.

(115) Luk'Yanchuk, B.; Zheludev, N. I.; Maier, S. A.; Halas, N. J.; Nordlander, P.; Giessen, H.; Chong, C. T. The Fano resonance in plasmonic nanostructures and metamaterials. *Nat. Mater.* **2010**, *9* (9), 707−715.

(116) Wang, K.; Huang, K.; Jiang, G. Enhanced removal of aqueous acetaminophen by a laccase-catalyzed oxidative coupling reaction under a dual-pH optimization strategy. *Sci. Total Environ.* **2018**, *616*, 1270−1278.

(117) Ferreira, P. C.; Ataide, V. N.; Silva Chagas, C. L.; Angnes, L.; Tomazelli Coltro, W. K.; Longo Cesar Paixao, T. R.; Reis de Araujo, W. Wearable electrochemical sensors for forensic and clinical applications. *TrAC, Trends Anal. Chem.* **2019**, *119*, 115622.

(118) Ray, T. R.; Choi, J.; Bandodkar, A. J.; Krishnan, S.; Gutruf, P.; Tian, L.; Ghaffari, R.; Rogers, J. A. Bio-integrated wearable systems: a comprehensive review. *Chem. Rev.* **2019**, *119* (8), 5461−5533.

(119) Ding, F.; Yang, Y.; Deshpande, R. A.; Bozhevolnyi, S. I. A review of gap-surface plasmon metasurfaces: fundamentals and applications. *Nanophotonics* **2018**, *7* (6), 1129−1156.

(120) Deshpande, R. A.; Ding, F.; Bozhevolnyi, S. Dual-band metasurfaces using multiple gap-surface plasmon resonances. *ACS Appl. Mater. Interfaces* **2020**, *12* (1), 1250−1256.

(121) High, A. A.; Devlin, R. C.; Dibos, A.; Polking, M.; Wild, D. S.; Perczel, J.; De Leon, N. P.; Lukin, M. D.; Park, H. Visible-frequency hyperbolic metasurface. *Nature* **2015**, *522* (7555), 192−196.

(122) Takayama, O.; Lavrinenko, A. V. Optics with hyperbolic materials. *JOSA B* **2019**, *36* (8), F38−F48.

(123) Huo, P.; Zhang, S.; Liang, Y.; Lu, Y.; Xu, T. Hyperbolic metamaterials and metasurfaces: fundamentals and applications. *Adv. Opt. Mater.* **2019**, *7* (14), 1801616.

(124) Decker, M.; Staude, I.; Falkner, M.; Dominguez, J.; Neshev, D. N.; Brener, I.; Pertsch, T.; Kivshar, Y. S. High-efficiency dielectric Huygens' surfaces. *Adv. Opt. Mater.* **2015**, *3* (6), 813−820.

(125) Yang, Q.; Kruk, S.; Xu, Y.; Wang, Q.; Srivastava, Y. K.; Koshelev, K.; Kravchenko, I.; Singh, R.; Han, J.; Kivshar, Y.; Shadrivov, I. Mie-resonant membrane huygens' metasurfaces. *Adv. Funct. Mater.* **2020**, *30* (4), 1906851.

(126) Leitis, A.; Heßler, A.; Wahl, S.; Wuttig, M.; Taubner, T.; Tittl, A.; Altug, H. All-dielectric programmable Huygens' metasurfaces. *Adv. Funct. Mater.* **2020**, *30* (19), 1910259.

(127) Arbabi, A.; Horie, Y.; Bagheri, M.; Faraon, A. Dielectric metasurfaces for complete control of phase and polarization with subwavelength spatial resolution and high transmission. *Nat. Nanotechnol.* **2015**, *10* (11), 937−943.

(128) Qiao, P.; Yang, W.; Chang-Hasnain, C. J. Recent advances in high-contrast metastructures, metasurfaces, and photonic crystals. *Adv. Opt. Photonics* **2018**, *10* (1), 180−245.

(129) Li, J.; Zhang, Y.; Li, J.; Yan, X.; Liang, L.; Zhang, Z.; Huang, J.; Li, J.; Yang, Y.; Yao, J. Amplitude modulation of anomalously reflected terahertz beams using all-optical active Pancharatnam−Berry coding metasurfaces. *Nanoscale* **2019**, *11* (12), 5746−5753.

(130) Khorasaninejad, M.; Chen, W.; Zhu, A.; Oh, J.; Devlin, R.; Rousso, D.; Capasso, F. Multispectral chiral imaging with a metalens. *Nano Lett.* **2016**, *16* (7), 4595−4600.

(131) Li, Z.; Zhang, T.; Wang, Y.; Kong, W.; Zhang, J.; Huang, Y.; Wang, C.; Li, X.; Pu, M.; Luo, X. Achromatic Broadband super-resolution imaging by super-oscillatory metasurface. *Laser Photonics Rev.* **2018**, *12* (10), 1800064.

(132) Zheng, P.; Dai, Q.; Li, Z.; Ye, Z.; Xiong, J.; Liu, H.-C.; Zheng, G.; Zhang, S. Metasurface-based key for computational imaging encryption. *Sci. Adv.* **2021**, *7* (21), eabg0363.

(133) Arbabi, E.; Li, J.; Hutchins, R. J.; Kamali, S. M.; Arbabi, A.; Horie, Y.; Van Dorpe, P.; Gradinaru, V.; Wagenaar, D. A.; Faraon, A. Two-photon microscopy with a double-wavelength metasurface objective lens. *Nano Lett.* **2018**, *18* (8), 4943−4948.

(134) Chen, W. T.; Zhu, A. Y.; Khorasaninejad, M.; Shi, Z.; Sanjeev, V.; Capasso, F. Immersion meta-lenses at visible wavelengths for nanoscale imaging. *Nano Lett.* **2017**, *17* (5), 3188−3194.

(135) Pahlevaninezhad, H.; Khorasaninejad, M.; Huang, Y.-W.; Shi, Z.; Hariri, L. P.; Adams, D. C.; Ding, V.; Zhu, A.; Qiu, C.-W.; Capasso, F.; Suter, M. J. Nano-optic endoscope for high-resolution optical coherence tomography *in vivo*. *Nat. Photonics* **2018**, *12* (9), 540−547.

(136) Slobozhanyuk, A. P.; Poddubny, A. N.; Raaijmakers, A. J.; van den Berg, C. A.; Kozachenko, A. V.; Dubrovina, I. A.; Melchakova, I. V.; Kivshar, Y. S.; Belov, P. A. Enhancement of magnetic resonance imaging with metasurfaces. *Adv. Mater.* **2016**, *28* (9), 1832−1838.

(137) Shchelokova, A. V.; Slobozhanyuk, A. P.; de Bruin, P.; Zivkovic, I.; Kallos, E.; Belov, P. A.; Webb, A. Experimental investigation of a metasurface resonator for *in vivo* imaging at 1.5 T. *J. Magn. Reson.* **2018**, *286*, 78−81.

(138) Schmidt, R.; Slobozhanyuk, A.; Belov, P.; Webb, A. Flexible and compact hybrid metasurfaces for enhanced ultra high field *in vivo* magnetic resonance imaging. *Sci. Rep.* **2017**, *7* (1), 1−7.

(139) Gollub, J.; Yurduseven, O.; Trofatter, K. P.; Arnitz, D.; Imani, M. F.; Sleasman, T.; Boyarsky, M.; Rose, A.; Pedross-Engel, A.; Odabasi, H.; Zvolensky, T.; Lipworth, G.; Brady, D.; Marks, D. L.; Reynolds, M. S.; Smith, D. R. Large metasurface aperture for millimeter wave computational imaging at the human-scale. *Sci. Rep.* **2017**, *7* (1), 1−9.

(140) Li, L.; Ruan, H.; Liu, C.; Li, Y.; Shuang, Y.; Alù, A.; Qiu, C.-W.; Cui, T. J. Machine-learning reprogrammable metasurface imager. *Nat. Commun.* **2019**, *10* (1), 1−8.

(141) Li, L.; Shuang, Y.; Ma, Q.; Li, H.; Zhao, H.; Wei, M.; Liu, C.; Hao, C.; Qiu, C.-W.; Cui, T. J. Intelligent metasurface imager and recognizer. *Light: Sci. Appl.* **2019**, *8* (1), 1−9.

(142) Lee, G.-H.; Moon, H.; Kim, H.; Lee, G. H.; Kwon, W.; Yoo, S.; Myung, D.; Yun, S. H.; Bao, Z.; Hahn, S. K. Multifunctional materials for implantable and wearable photonic healthcare devices. *Nat. Rev. Mater.* **2020**, *5* (2), 149−165.

(143) Chen, L. Y.; Tee, B. C.-K.; Chortos, A. L.; Schwartz, G.; Tse, V.; Lipomi, D. J.; Wong, H.-S. P.; McConnell, M. V.; Bao, Z. Continuous wireless pressure monitoring and mapping with ultra-small passive sensors for health monitoring and critical care. *Nat. Commun.* **2014**, *5* (1), 1−10.

(144) Dautta, M.; Alshetaiwi, M.; Escobar, A.; Torres, F.; Bernardo, N.; Tseng, P. Multi-functional hydrogel-interlayer RF/NFC resonators as a versatile platform for passive and wireless biosensing. *Adv. Electron. Mater.* **2020**, *6* (4), 1901311.

(145) Zhang, C.; Dong, H.; Zhang, C.; Fan, Y.; Yao, J.; Zhao, Y. S. Photonic skins based on flexible organic microlaser arrays. *Sci. Adv.* **2021**, *7* (31), eabh3530.

(146) Pendry, J. B.; Schurig, D.; Smith, D. R. Controlling electromagnetic fields. *Science* **2006**, *312* (5781), 1780−1782.

(147) Leonhardt, U. Optical conformal mapping. *Science* **2006**, *312* (5781), 1777−1780.

(148) Schurig, D.; Mock, J. J.; Justice, B.; Cummer, S. A.; Pendry, J. B.; Starr, A. F.; Smith, D. R. Metamaterial electromagnetic cloak at microwave frequencies. *Science* **2006**, *314* (5801), 977−980.

(149) Li, J.; Pendry, J. B. Hiding under the carpet: a new strategy for cloaking. *Phys. Rev. Lett.* **2008**, *101* (20), 203901.

(150) Liu, R.; Ji, C.; Mock, J.; Chin, J.; Cui, T.; Smith, D. Broadband ground-plane cloak. *Science* **2009**, *323* (5912), 366−369.

(151) Ergin, T.; Stenger, N.; Brenner, P.; Pendry, J. B.; Wegener, M. Three-dimensional invisibility cloak at optical wavelengths. *Science* **2010**, *328* (5976), 337−339.

(152) Selvanayagam, M.; Eleftheriades, G. V. Experimental demonstration of active electromagnetic cloaking. *Physical review X* **2013**, *3* (4), No. 041011.

(153) Chu, H.; Li, Q.; Liu, B.; Luo, J.; Sun, S.; Hang, Z. H.; Zhou, L.; Lai, Y. A hybrid invisibility cloak based on integration of transparent metasurfaces and zero-index materials. *Light: Sci. Appl.* **2018**, *7* (1), 1−8.

(154) Zhang, S.; Xia, C.; Fang, N. Broadband acoustic cloak for ultrasound waves. *Phys. Rev. Lett.* **2011**, *106* (2), No. 024301.

(155) Stenger, N.; Wilhelm, M.; Wegener, M. Experiments on elastic cloaking in thin plates. *Phys. Rev. Lett.* **2012**, *108* (1), No. 014301.

(156) Yang, F.; Mei, Z. L.; Jin, T. Y.; Cui, T. J. DC electric invisibility cloak. *Phys. Rev. Lett.* **2012**, *109* (5), No. 053902.

(157) Park, J.; Youn, J. R.; Song, Y. S. Hydrodynamic Metamaterial Cloak for Drag-Free Flow. *Phys. Rev. Lett.* **2019**, *123* (7), No. 074502.

(158) Bückmann, T.; Thiel, M.; Kadic, M.; Schittny, R.; Wegener, M. An elasto-mechanical unfeelability cloak made of pentamode metamaterials. *Nat. Commun.* **2014**, *5*, 4130.

(159) Bückmann, T.; Kadic, M.; Schittny, R.; Wegener, M. Mechanical cloak design by direct lattice transformation. *Proc. Natl. Acad. Sci. U. S. A.* **2015**, *112* (16), 4930−4934.

(160) Schittny, R.; Kadic, M.; Guenneau, S.; Wegener, M. Experiments on transformation thermodynamics: molding the flow of heat. *Phys. Rev. Lett.* **2013**, *110* (19), 195901.

(161) Yan, Z.; Xu, D.; Lin, Z.; Wang, P.; Cao, B.; Ren, H.; Song, F.; Wan, C.; Wang, L.; Zhou, J.; Zhao, X.; Chen, J.; Huang, Y.; Duan, X. Highly stretchable van der Waals thin films for adaptable and breathable electronic membranes. *Science* **2022**, *375* (6583), 852−859.

(162) Zan, G.; Wu, T.; Zhang, Z.; Li, J.; Zhou, J.; Zhu, F.; Chen, H.; Wen, M.; Yang, X.; Peng, X.; Chen, J.; Wu, Q. Bioinspired Nanocomposites with Self-Adaptive Stress Dispersion for Super-Foldable Electrodes. *Adv. Sci.* **2022**, *9* (3), 2103714.

(163) Pu, S.; Fu, J.; Liao, Y.; Ge, L.; Zhou, Y.; Zhang, S.; Zhao, S.; Liu, X.; Hu, X.; Liu, K.; Chen, J. Promoting energy efficiency via a self-adaptive evaporative cooling hydrogel. *Adv. Mater.* **2020**, *32* (17), 1907307.

(164) Zhu, G.; Zhou, Y. S.; Bai, P.; Meng, X. S.; Jing, Q.; Chen, J.; Wang, Z. L. A shape-adaptive thin-film-based approach for 50% high-efficiency energy generation through micro-grating sliding electrification. *Adv. Mater.* **2014**, *26* (23), 3788−3796.

(165) Ee, H.-S.; Agarwal, R. Tunable metasurface and flat optical zoom lens on a stretchable substrate. *Nano Lett.* **2016**, *16* (4), 2818−2823.

(166) Zhu, W.; Song, Q.; Yan, L.; Zhang, W.; Wu, P.-C.; Chin, L. K.; Cai, H.; Tsai, D. P.; Shen, Z. X.; Deng, T. W.; et al. A flat lens with tunable phase gradient by using random access reconfigurable metamaterial. *Adv. Mater.* **2015**, *27* (32), 4739−4743.

(167) Ma, X.; Zhang, M.; Zhang, J.; Wang, S.; Cao, S.; Li, Y.; Hu, G.; Kong, D. Highly permeable and ultrastretchable liquid metal micromesh for skin-attachable electronics. *ACS Materials Lett.* **2022**, *4* (4), 634−641.

(168) Zhu, H.; Wang, S.; Zhang, M.; Li, T.; Hu, G.; Kong, D. Fully solution processed liquid metal features as highly conductive and ultrastretchable conductors. *npj Flex. Electron.* **2021**, *5* (1), 25.

(169) Li, Y.; Fang, T.; Zhang, J.; Zhu, H.; Sun, Y.; Wang, S.; Lu, Y.; Kong, D. Ultrasensitive and ultrastretchable electrically self-healing conductors. *Proc. Natl. Acad. Sci. U. S. A.* **2023**, *120* (23), e2300953120.

(170) Tang, Y.; Lin, G.; Yang, S.; Yi, Y. K.; Kamien, R. D.; Yin, J. Programmable Kiri-Kirigami metamaterials. *Adv. Mater.* **2017**, *29* (10), 1604262.

(171) Zheng, Y.; Chen, K.; Yang, W.; Wu, L.; Qu, K.; Zhao, J.; Jiang, T.; Feng, Y. Kirigami Reconfigurable Gradient Metasurface. *Adv. Funct. Mater.* **2022**, *32* (5), 2107699.

(172) Moccia, M.; Liu, S.; Wu, R. Y.; Castaldi, G.; Andreone, A.; Cui, T. J.; Galdi, V. Coding metasurfaces for diffuse scattering: scaling laws, bounds, and suboptimal design. *Adv. Opt. Mater.* **2017**, *5* (19), 1700455.
(173) Wu, R. Y.; Shi, C. B.; Liu, S.; Wu, W.; Cui, T. J. Addition theorem for digital coding metamaterials. *Adv. Opt. Mater.* **2018**, *6* (5), 1701236.
(174) Luo, Z.; Wang, Q.; Zhang, X. G.; Wu, J. W.; Dai, J. Y.; Zhang, L.; Wu, H. T.; Zhang, H. C.; Ma, H. F.; Cheng, Q.; Cui, T. J. Intensity-dependent metasurface with digitally reconfigurable distribution of nonlinearity. *Adv. Opt. Mater.* **2019**, *7* (19), 1900792.
(175) Zhang, L.; Chen, X. Q.; Shao, R. W.; Dai, J. Y.; Cheng, Q.; Castaldi, G.; Galdi, V.; Cui, T. J. Breaking reciprocity with space-time-coding digital metasurfaces. *Adv. Mater.* **2019**, *31* (41), 1904069.
(176) Ma, Q.; Chen, L.; Jing, H. B.; Hong, Q. R.; Cui, H. Y.; Liu, Y.; Li, L.; Cui, T. J. Controllable and programmable nonreciprocity based on detachable digital coding metasurface. *Adv. Opt. Mater.* **2019**, *7* (24), 1901285.
(177) Jing, H. B.; Ma, Q.; Bai, G. D.; Cui, T. J. Anomalously Perfect Reflections Based on 3-Bit Coding Metasurfaces. *Adv. Opt. Mater.* **2019**, *7* (9), 1801742.
(178) Zhang, L.; Wang, Z. X.; Shao, R. W.; Shen, J. L.; Chen, X. Q.; Wan, X.; Cheng, Q.; Cui, T. J. Dynamically realizing arbitrary multi-bit programmable phases using a 2-bit time-domain coding metasurface. *IEEE Trans. Antennas Propag.* **2020**, *68* (4), 2984−2992.
(179) Qiu, T.; Shi, X.; Wang, J.; Li, Y.; Qu, S.; Cheng, Q.; Cui, T.; Sui, S. Deep learning: a rapid and efficient route to automatic metasurface design. *Adv. Sci.* **2019**, *6* (12), 1900128.
(180) Zhu, R.; Wang, J.; Qiu, T.; Han, Y.; Fu, X.; Shi, Y.; Liu, X.; Liu, T.; Zhang, Z.; Chu, Z.; Qiu, C.-W.; Qu, S. Remotely mind-controlled metasurface via brainwaves. *eLight* **2022**, *2* (1), 1−11.
(181) Moeini, S.; Cui, T. J. Fractal coding metamaterials. *Ann. Phys.* **2019**, *531* (2), 1800134.
(182) Zhao, J.; Yang, X.; Dai, J. Y.; Cheng, Q.; Li, X.; Qi, N. H.; Ke, J. C.; Bai, G. D.; Liu, S.; Jin, S.; Alù, A.; Cui, T. J. Programmable time-domain digital-coding metasurface for non-linear harmonic manipulation and new wireless communication systems. *Natl. Sci. Rev.* **2019**, *6* (2), 231−238.
(183) Wu, H.; Liu, S.; Wan, X.; Zhang, L.; Wang, D.; Li, L.; Cui, T. J. Controlling energy radiations of electromagnetic waves via frequency coding metamaterials. *Adv. Sci.* **2017**, *4* (9), 1700098.
(184) Zhang, L.; Chen, X. Q.; Liu, S.; Zhang, Q.; Zhao, J.; Dai, J. Y.; Bai, G. D.; Wan, X.; Cheng, Q.; Castaldi, G. Space-time-coding digital metasurfaces. *Nat. Commun.* **2018**, *9* (1), 1−11.
(185) Wan, X.; Wang, J. W.; Huang, Z. A.; Li, B. Y.; Xiao, Q.; Cui, T. J. Space−Time−Frequency Modulation Mechanisms of Monochromatic and Nonmonochromatic Electromagnetic Waves on a Digital Programmable Transmission Metasurface. *Adv. Funct. Mater.* **2022**, *32* (13), 2107557.
(186) Zhang, X. G.; Yu, Q.; Jiang, W. X.; Sun, Y. L.; Bai, L.; Wang, Q.; Qiu, C. W.; Cui, T. J. Polarization-controlled dual-programmable metasurfaces. *Adv. Sci.* **2020**, *7* (11), 1903382.
(187) Bao, L.; Fu, X.; Wu, R. Y.; Ma, Q.; Cui, T. J. Full-Space Manipulations of Electromagnetic Wavefronts at Two Frequencies by Encoding Both Amplitude and Phase of Metasurface. *Adv. Mater. Technol.* **2021**, *6* (4), 2001032.
(188) Xu, P.; Tian, H. W.; Jiang, W. X.; Chen, Z. Z.; Cao, T.; Qiu, C. W.; Cui, T. J. Phase and polarization modulations using radiation-type metasurfaces. *Adv. Opt. Mater.* **2021**, *9* (16), 2100159.
(189) Wu, G.-B.; Dai, J. Y.; Cheng, Q.; Cui, T. J.; Chan, C. H. Sideband-free space−time-coding metasurface antennas. *Nat. Electron.* **2022**, *5*, 808−819.
(190) Wang, Z. X.; Wu, J. W.; Wu, L. W.; Gou, Y.; Ma, H. F.; Cheng, Q.; Cui, T. J. High efficiency polarization-encoded holograms with ultrathin bilayer spin-decoupled information metasurfaces. *Adv. Opt. Mater.* **2021**, *9* (5), 2001609.
(191) Zhang, X. G.; Sun, Y. L.; Yu, Q.; Cheng, Q.; Jiang, W. X.; Qiu, C. W.; Cui, T. J. Smart Doppler cloak operating in broad band and full polarizations. *Adv. Mater.* **2021**, *33* (17), 2007966.
(192) Chen, T.; Zheng, B.; Yang, Y.; Shen, L.; Wang, Z.; Gao, F.; Li, E.; Luo, Y.; Cui, T. J.; Chen, H. Direct current remote cloak for arbitrary objects. *Light: Sci. Appl.* **2019**, *8* (1), 1−6.
(193) Rajabalipanah, H.; Abdolali, A.; Iqbal, S.; Zhang, L.; Cui, T. J. Analog signal processing through space-time digital metasurfaces. *Nanophotonics* **2021**, *10* (6), 1753−1764.
(194) You, J. W.; Ma, Q.; Lan, Z.; Xiao, Q.; Panoiu, N. C.; Cui, T. J. Reprogrammable plasmonic topological insulators with ultrafast control. *Nat. Commun.* **2021**, *12* (1), 1−7.
(195) Zhang, L.; Chen, M. Z.; Tang, W.; Dai, J. Y.; Miao, L.; Zhou, X. Y.; Jin, S.; Cheng, Q.; Cui, T. J. A wireless communication scheme based on space-and frequency-division multiplexing using digital metasurfaces. *Nat. Electron.* **2021**, *4* (3), 218−227.
(196) Wang, H. P.; Zhou, Y. X.; Li, H.; Liu, G. D.; Yin, S. M.; Li, P. J.; Dong, S. Y.; Gong, C. Y.; Wang, S. Y.; Li, Y. B.; Cui, T. J. Noncontact Electromagnetic Wireless Recognition for Prosthesis Based on Intelligent Metasurface. *Adv. Sci.* **2022**, *9*, 2105056.
(197) Han, J.; Li, L.; Ma, X.; Gao, X.; Mu, Y.; Liao, G.; Luo, Z. J.; Cui, T. J. Adaptively smart wireless power transfer using 2-bit programmable metasurface. *IEEE Transactions on Industrial Electronics* **2022**, *69* (8), 8524−8534.
(198) Liu, C. X.; Yang, F.; Fu, X. J.; Wu, J. W.; Zhang, L.; Yang, J.; Cui, T. J. Programmable manipulations of terahertz beams by transmissive digital coding metasurfaces based on liquid crystals. *Adv. Opt. Mater.* **2021**, *9* (22), 2100932.
(199) Li, Z.; Fei, C.; Yang, S.; Hou, C.; Zhao, J.; Li, Y.; Zheng, C.; Wu, H.; Quan, Y.; Zhao, T.; et al. Coding Piezoelectric Metasurfaces. *Adv. Funct. Mater.* **2022**, *32*, 2209173.
(200) Liu, S.; Cui, T. J. Concepts, working principles, and applications of coding and programmable metamaterials. *Adv. Opt. Mater.* **2017**, *5* (22), 1700624.
(201) Abadal, S.; Cui, T.-J.; Low, T.; Georgiou, J. Programmable metamaterials for software-defined electromagnetic control: Circuits, systems, and architectures. *IEEE Journal on Emerging and Selected Topics in Circuits and Systems* **2020**, *10* (1), 6−19.
(202) Tian, H. W.; Shen, H. Y.; Zhang, X. G.; Li, X.; Jiang, W. X.; Cui, T. J. Terahertz metasurfaces: toward multifunctional and programmable wave manipulation. *Front. Phys.* **2020**, *8*, 584077.
(203) Zhang, L.; Cui, T. J. Space-time-coding digital metasurfaces: Principles and applications. *Research* **2021**, DOI: 10.34133/2021/9802673.
(204) Saifullah, Y.; He, Y.; Boag, A.; Yang, G. M.; Xu, F. Recent Progress in Reconfigurable and Intelligent Metasurfaces: A Comprehensive Review of Tuning Mechanisms, Hardware Designs, and Applications. *Adv. Sci.* **2022**, *9*, 2203747.
(205) Aksu, S.; Huang, M.; Artar, A.; Yanik, A. A.; Selvarasah, S.; Dokmeci, M. R.; Altug, H. Flexible plasmonics on unconventional and nonplanar substrates. *Adv. Mater.* **2011**, *23* (38), 4422−4430.
(206) Cheng, J.; Jafar-Zanjani, S.; Mosallaei, H. All-dielectric ultrathin conformal metasurfaces: lensing and cloaking applications at 532 nm wavelength. *Sci. Rep.* **2016**, *6* (1), 1−10.
(207) Jiang, Z. H.; Yun, S.; Toor, F.; Werner, D. H.; Mayer, T. S. Conformal dual-band near-perfectly absorbing mid-infrared metamaterial coating. *ACS Nano* **2011**, *5* (6), 4641−4647.
(208) Chen, H.; Yang, X.; Wu, S.; Zhang, D.; Xiao, H.; Huang, K.; Zhu, Z.; Yuan, J. Flexible and conformable broadband metamaterial absorber with wide-angle and polarization stability for radar application. *Mater. Res. Express* **2018**, *5* (1), No. 015804.
(209) Zhang, M.; Ma, X.; Pu, M.; Liu, K.; Guo, Y.; Huang, Y.; Xie, X.; Li, X.; Yu, H.; Luo, X. Large-Area and Low-Cost Nanoslit-Based Flexible Metasurfaces for Multispectral Electromagnetic Wave Manipulation. *Adv. Opt. Mater.* **2019**, *7* (23), 1900657.
(210) Li, J.; Zhang, L.; Zhang, M.; Su, H.; Li, I. L.; Ruan, S.; Liang, H. Wearable conformal metasurfaces for polarization division multiplexing. *Adv. Opt. Mater.* **2020**, *8* (13), 2000068.
(211) Jang, Y.; Yoo, M.; Lim, S. Conformal metamaterial absorber for curved surface. *Opt. Express* **2013**, *21* (20), 24163−24170.

(212) Zheng, Y.; Chen, K.; Jiang, T.; Zhao, J.; Feng, Y. Multi-octave microwave absorption via conformal metamaterial absorber with optical transparency. *J. Phys. D Appl. Phys.* **2019**, *52* (33), 335101.
(213) Teo, J. Y. H.; Wong, L. J.; Molardi, C.; Genevet, P. Controlling electromagnetic fields at boundaries of arbitrary geometries. *Phys. Rev. A* **2016**, *94* (2), No. 023820.
(214) Xu, H.-X.; Hu, G.; Wang, Y.; Wang, C.; Wang, M.; Wang, S.; Huang, Y.; Genevet, P.; Huang, W.; Qiu, C.-W. Polarization-insensitive 3D conformal-skin metasurface cloak. *Light: Sci. Appl.* **2021**, *10* (1), 1−13.
(215) Wang, C.; Lv, Z.; Mohan, M. P.; Cui, Z.; Liu, Z.; Jiang, Y.; Li, J.; Wang, C.; Pan, S.; Karim, M. F.; Liu, A. Q.; Chen, X. Pangolin-Inspired Stretchable, Microwave-Invisible Metascale. *Adv. Mater.* **2021**, *33* (41), 2102131.
(216) Choi, G. P. T.; Dudte, L. H.; Mahadevan, L. Programming shape using kirigami tessellations. *Nat. Mater.* **2019**, *18* (9), 999−1004.
(217) Lee, Y.-K.; Xi, Z.; Lee, Y.-J.; Kim, Y.-H.; Hao, Y.; Choi, H.; Lee, M.-G.; Joo, Y.-C.; Kim, C.; Lien, J.-M.; Choi, I.-S. Computational wrapping: A universal method to wrap 3D-curved surfaces with nonstretchable materials for conformal devices. *Sci. Adv.* **2020**, *6* (15), eaax6212.
(218) Jin, L.; Yeager, M.; Lee, Y.-J.; O'Brien, D. J.; Yang, S. Shape-morphing into 3D curved surfaces with nacre-like composite architectures. *Sci. Adv.* **2022**, *8* (41), eabq3248.
(219) Konaković, M.; Crane, K.; Deng, B.; Bouaziz, S.; Piker, D.; Pauly, M. Beyond developable: computational design and fabrication with auxetic materials. *ACM Trans. Graph.* **2016**, *35* (4), 1−11.
(220) Konaković-Luković, M.; Panetta, J.; Crane, K.; Pauly, M. Rapid deployment of curved surfaces via programmable auxetics. *ACM Trans. Graph.* **2018**, *37* (4), 1−13.
(221) Jiang, C.; Rist, F.; Wang, H.; Wallner, J.; Pottmann, H. Shape-morphing mechanical metamaterials. *Comput.-Aided Des.* **2022**, *143*, 103146.
(222) Liu, J.; Jiang, S.; Xiong, W.; Zhu, C.; Li, K.; Huang, Y. Self-Healing Kirigami Assembly Strategy for Conformal Electronics. *Adv. Funct. Mater.* **2022**, *32* (12), 2109214.
(223) Jiang, S.; Liu, J.; Xiong, W.; Yang, Z.; Yin, L.; Li, K.; Huang, Y. A Snakeskin-Inspired, Soft-Hinge Kirigami Metamaterial for Self-Adaptive Conformal Electronic Armor. *Adv. Mater.* **2022**, *34* (31), 2204091.
(224) Meitl, M. A.; Zhu, Z.-T.; Kumar, V.; Lee, K. J.; Feng, X.; Huang, Y. Y.; Adesida, I.; Nuzzo, R. G.; Rogers, J. A. Transfer printing by kinetic control of adhesion to an elastomeric stamp. *Nat. Mater.* **2006**, *5* (1), 33−38.
(225) Le Borgne, B.; Liu, S.; Morvan, X.; Crand, S.; Sporea, R. A.; Lu, N.; Harnois, M. Water Transfer Printing Enhanced by Water-Induced Pattern Expansion: Toward Large-Area 3D Electronics. *Adv. Mater. Technol.* **2019**, *4* (4), 1800600.
(226) Park, H.; Cho, H.; Kim, J.; Bang, J. W.; Seo, S.; Rahmawan, Y.; Lee, D. Y.; Suh, K. Y. Multiscale transfer printing into recessed microwells and on curved surfaces via hierarchical perfluoropolyether stamps. *Small* **2014**, *10* (1), 52−59.
(227) Sim, K.; Chen, S.; Li, Z.; Rao, Z.; Liu, J.; Lu, Y.; Jang, S.; Ershad, F.; Chen, J.; Xiao, J.; Yu, C. Three-dimensional curvy electronics created using conformal additive stamp printing. *Nat. Electron.* **2019**, *2* (10), 471−479.
(228) Alkadi, F.; Lee, K.-C.; Bashiri, A. H.; Choi, J.-W. Conformal additive manufacturing using a direct-print process. *Addit. Manuf.* **2020**, *32*, 100975.
(229) Kucukdeger, E.; Tong, Y.; Singh, M.; Zhang, J.; Harding, L. K.; Salado, A.; Ellingson, S. W.; Johnson, B. N. Conformal 3D printing of non-planar antennas on wrinkled and folded kapton films using point cloud data. *Flexible Printed Electron.* **2021**, *6* (4), No. 044002.
(230) Huang, Y.; Wu, H.; Zhu, C.; Xiong, W.; Chen, F.; Xiao, L.; Liu, J.; Wang, K.; Li, H.; Ye, D.; Duan, Y.; Chen, J.; Yang, H.; Li, W.; Bai, K.; Yin, Z.; Ding, H. Programmable robotized 'transfer-and-jet'printing for large, 3D curved electronics on complex surfaces. *Int. J. Extreme Manuf.* **2021**, *3* (4), No. 045101.
(231) Zhang, K. P.; Liao, Y. F.; Qiu, B.; Zheng, Y. K.; Yu, L. K.; He, G. H.; Chen, Q. N.; Sun, D. H. 3d printed embedded metamaterials. *Small* **2021**, *17* (50), 2103262.
(232) Gu, X.; Luo, F.; Yau, S. T. Computational conformal geometry behind modern technologies. *Not. Am. Math. Soc.* **2020**, *67* (10), 1509−1525.
(233) Chen, Z.; Guo, Q.; Majidi, C.; Chen, W.; Srolovitz, D. J.; Haataja, M. P. Nonlinear geometric effects in mechanical bistable morphing structures. *Phys. Rev. Lett.* **2012**, *109* (11), 114302.
(234) Lin, H.; Sturmberg, B. C.; Lin, K.-T.; Yang, Y.; Zheng, X.; Chong, T. K.; de Sterke, C. M.; Jia, B. A 90-nm-thick graphene metamaterial for strong and extremely broadband absorption of unpolarized light. *Nat. Photonics* **2019**, *13* (4), 270−276.
(235) Wang, K.; Wu, C.; Wang, F.; Liu, C.; Yu, C.; Jiang, G. In situ insertion of carbon nanotubes into metal-organic frameworks-derived α-Fe2O3 polyhedrons for highly sensitive electrochemical detection of nitrite. *Electrochim. Acta* **2018**, *285*, 128−138.
(236) Cong, L.; Srivastava, Y. K.; Solanki, A.; Sum, T. C.; Singh, R. Perovskite as a platform for active flexible metaphotonic devices. *ACS Photonics* **2017**, *4* (7), 1595−1601.
(237) Zhao, H.; Shuang, Y.; Wei, M.; Cui, T. J.; Hougne, P. d.; Li, L. Metasurface-assisted massive backscatter wireless communication with commodity Wi-Fi signals. *Nat. Commun.* **2020**, *11* (1), 3926.

https://doi.org/10.1021/acsnano.3c09310
ACS Nano 2024, 18, 2685−2707